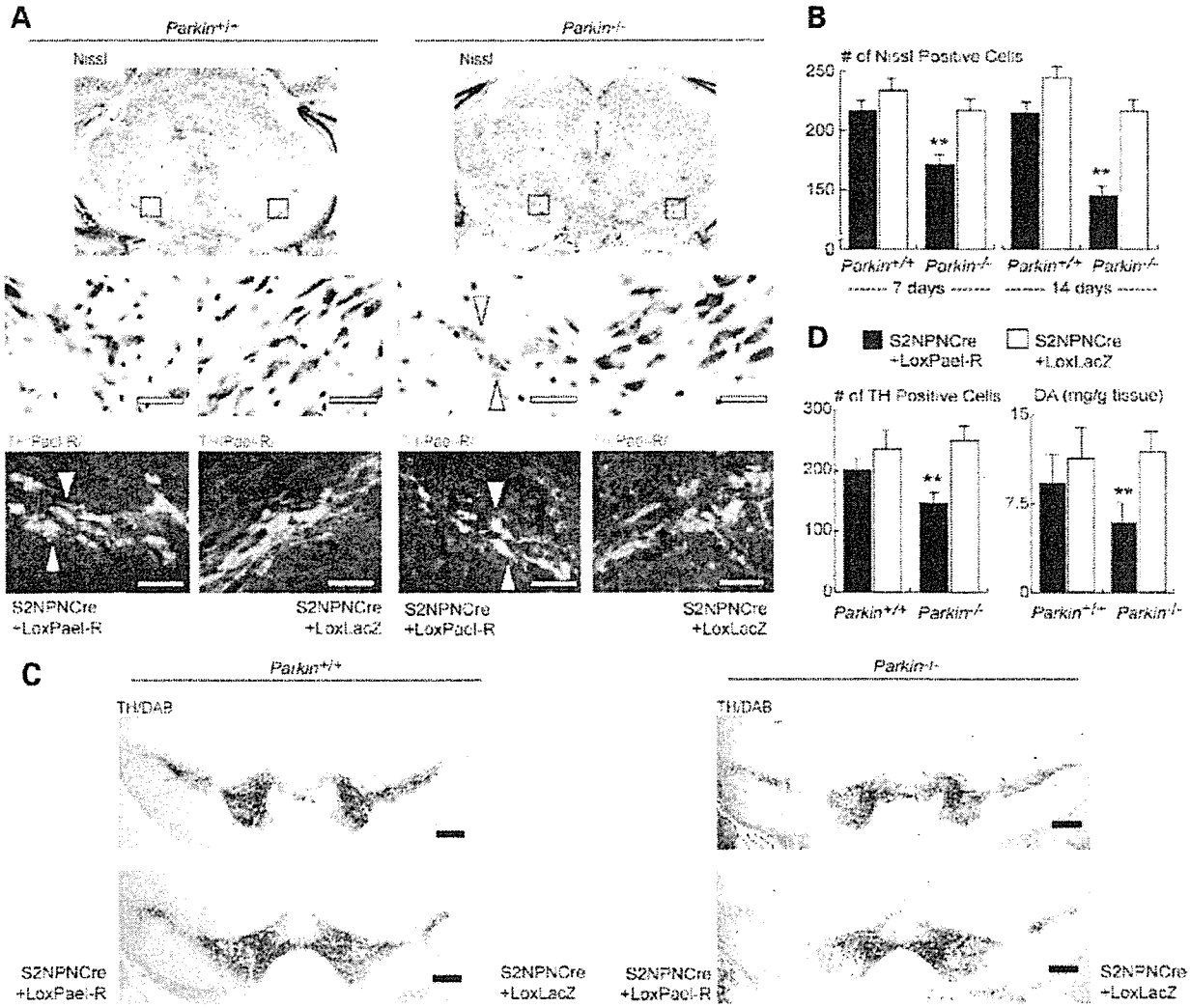

Figure 3. Enhanced neuronal death in the SNpc of parkin$^{-/-}$ mice by the up-regulation of Pael-R. (**A**) Adenoviral vectors (2 μl), including LoxEGFP (5×10^8 p.f.u.), S2NPNCre (10^9 p.f.u.) and LoxPael-R (10^9 p.f.u.) were injected unilaterally in the striatum of either parkin$^{+/+}$ or parkin$^{-/-}$ mice, as described in Figure 1. As a control, LoxPael-R was replaced by LoxLacZ (10^9 p.f.u.), and S2NPNCre + LoxLacZ was injected on the contralateral side. Brains of animals were then perfusion-fixed 7 days later, and midbrain sections were stained using the Nissl method (upper two panels). One of consecutive sections was also immunostained with anti-Pael-R antibody (lower panels). Images at −3.52 mM from the Bregma are shown. The open boxes in the upper panel are magnified in lower two panels. Typical examples of neurons positive with both TH and Pael-R are indicated by white arrowheads in the lower panels. Typical examples of degenerating neurons are identified by the open arrowheads in the middle panels. (**B**) Nissl positive neurons were counted on the ipsilateral (closed bars) and contralateral sides (open bars) as described in the text, 7 and 14 days after the injection. In each case, $n = 6$, and the mean ± SD is shown. ** denotes $P < 0.01$ compared to parkin$^{+/+}$ mice injected with LoxLacZ. (**C**) 10 days after the injection, midbrain sections were stained with anti-TH antibody as described in text. Images at −3.28 mM (upper panels) and −3.52 mM from the Bregma (lower panels) are shown. (**D**) TH positive neurons were counted 7 days after the injection (left panel). DA content was also measured by the HPLC-EC method 7 days after the injection (right panel). In each case, closed and open bars correspond to the ipsilateral (closed bars) or contralateral striatum (open bars) of parkin$^{-/-}$ or parkin$^{+/+}$ mice, respectively. In each case, $n = 6$, and the mean ± SD is shown. ** denotes $P < 0.01$ compared to parkin$^{+/+}$ mice injected with LoxLacZ.

side received injection of S2NPNCre, LoxPael-R and LoxEGFP) based on EGFP fluorescence or Nissl staining (Supplementary Material, Fig. S2B), diminished dopamine content most likely reflects loss of functional dopaminergic neurons in the ipsilateral SNpc. Moreover, injection of S2NPNCre and LoxPael-R resulted in the expression of Pael-R (marked by expression of EGFP) also in the motor cortex by retrograde infection (Supplementary Material, Fig. S2A). In contrast to the SNpc, no neuronal death was observed in either motor cortex or striatum (Supplementary Material, Fig. S2C). In other brain sublesions which have the connection to the striatum (i.e. the thalamus, the interpeduncular nucleus, the locus coeruleus and the raphe nucleus), no EGFP signals were detected, which may be due to the fewer communication to the striatum (not shown). The loss of TH immunointensity in the SNpc mainly occurred in neurons expressing Pael-R (Supplementary Material, Fig. S3A–C). These data suggest that Pael-R overexpression caused neuronal cell death, rather selectively in dopaminergic neurons in the SNpc.

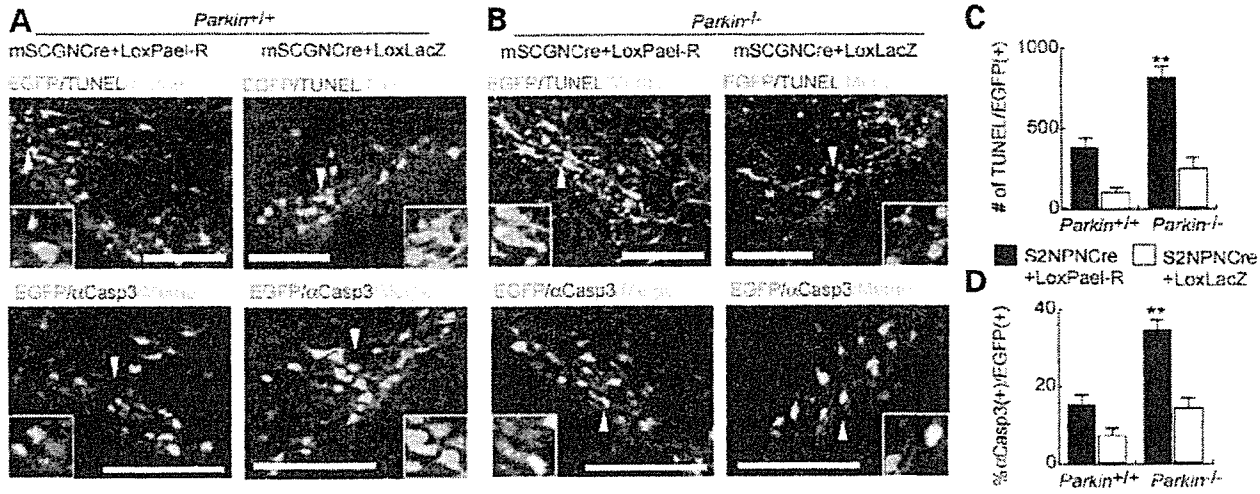

Figure 4. Assessment of neuronal cell death in parkin$^{-/-}$ mice (**A,B**) After infection of adenoviral vectors by the same protocol as used in Figure 3, brains of animals were perfusion-fixed 7 (upper panels for TUNEL) and 5 (lower panels for activated caspase-3 staining) days later, and midbrain sections were stained using either the TUNEL method or anti-activated caspase-3 antibody (αCasp3). Images at ~3.52 mM from the Bregma were obtained to visualize the indicated antibody and the EGFP signal (green). In each panel, areas indicated by arrowheads are magnified in the insets at the lower corner of the panel. Note that TUNEL-positive and activated caspase-3-positive cells are increased in the EGFP positive area. Scale bar: 200 μm. Images shown in this figure (panels A,B) are representative of six repeated experiments. (**C,D**) Quantitation of TUNEL-positive signals (number of positive signals) 7 days after injection (panel C) or the percentage of cells positive for activated caspase-3 (αCasp3) in the population of EGFP-positive neurons 5 days after injection (panel D) on the ipsilateral (closed bars) or contralateral SNpc (open bars) of either parkin$^{-/-}$ or parkin$^{+/+}$ mice. In each case, $n = 6$, and the mean ± SD is shown. ** denotes $P < 0.01$ compared to parkin$^{-/-}$ mice injected with LoxLacZ.

ORP150 suppresses Pael-R-mediated neuronal cell death

These observations led us to hypothesize that ER stress might trigger loss of dopaminergic neurons due to accumulation of toxic Pael-R. To gain further insight into mechanisms underlying this observation, we focused on the function of an ER chaperone, ORP150, which promotes protein folding/degradation (17). We reasoned that if the ER stress is the cause of Pael-R-mediated dopaminergic neuron death, even in the presence of wild-type *Parkin*, decreased levels of ORP150 should accentuate Pael-R-induced neuronal death in the SNpc, whereas overexpression of ORP150 might be protective. Using targeted injection of adenoviral vectors (as above), Pael-R was overexpressed in the SNpc of either heterozygous *Orp150* truncation mutants [*Orp150*$^{+/-}$ mice; note, homozygous *Orp150*$^{-/-}$ mice have a developmental lethal phenotype 13)], strain-matched controls (*Orp150*$^{+/+}$ mice) or *Orp150* overexpressing wild-type transgenics [*Orp150* TG mice, driven by pCAGGS promoter (21)]. Elevated levels of ORP150 were confirmed in SNpc neurons of *Orp150* TG mice by immunohistochemical analysis (Supplementary Material, Fig. S4 upper panels; levels of ORP150 in strain-matched normal animals are also shown in lower panels). Degeneration of dopaminergic neurons was assessed by TUNEL staining and expression of activated caspase-3 (Fig. 5A and B), since these methods appeared to have adequate sensitivity, as shown in Figure 4. A gene dosage effect was observed; increased levels of ORP150 afforded protection to dopaminergic neurons. *Orp150*$^{+/-}$ mice, with the lowest levels of functional ORP150, displayed exaggerated damage to dopaminergic neurons; TUNEL staining and activated caspase-3 were enhanced on the ipsilateral SNpc (the side in which injection of adenoviral vectors resulted in over-expression of Pael-R; Fig. 5A and B), whereas no significant cell death was observed on the contralateral side where LoxLacZ was expressed (data not shown). Each of these indices of neuronal stress/toxicity in this setting was decreased, in a manner dependent on the 'dose' of *Orp150*, when the same experiment was performed in wild-type (*Orp150*$^{+/+}$) or mice overexpressing ORP150 (*Orp150* TG mice) (Fig. 5A and B).

These data suggest an essential contribution of ER function in protecting neurons from lethal toxicity when Pael-R is overexpressed. According to this concept, we further reasoned that such neurons in *Parkin*$^{-/-}$ mice might be rescued by either expression of Parkin or ER chaperones capable of promoting protein folding/renaturation, such as GRP78. Though adenoviral expression of LacZ in neurons failed to rescue SNpc neurons from Pael-R-mediated cell death, overexpression of Parkin minimized neuronal damage (Fig. 5C). Similarly, overexpression of GRP78 could substitute for Parkin in preventing Pael-R-mediated neuronal death in *Parkin*$^{-/-}$ mice. Western blot analysis of brain stem samples confirmed the expression of transfected gene products (Fig. 5C, right panel). These data indicate that the ER chaperones, such as GRP78 and ORP150, have the capacity to relieve ER stress due to increased expression of Pael-R, thereby exerting a protective effect on dopaminergic neurons in the SNpc.

Suppression of Pael-R-mediated cell death by inhibition of dopamine synthesis

Increased dopamine content in the striatum of *Parkin*$^{-/-}$ mice has been noted by some investigators, though the increase is small (18,19). Furthermore, Pael-R has been implicated in

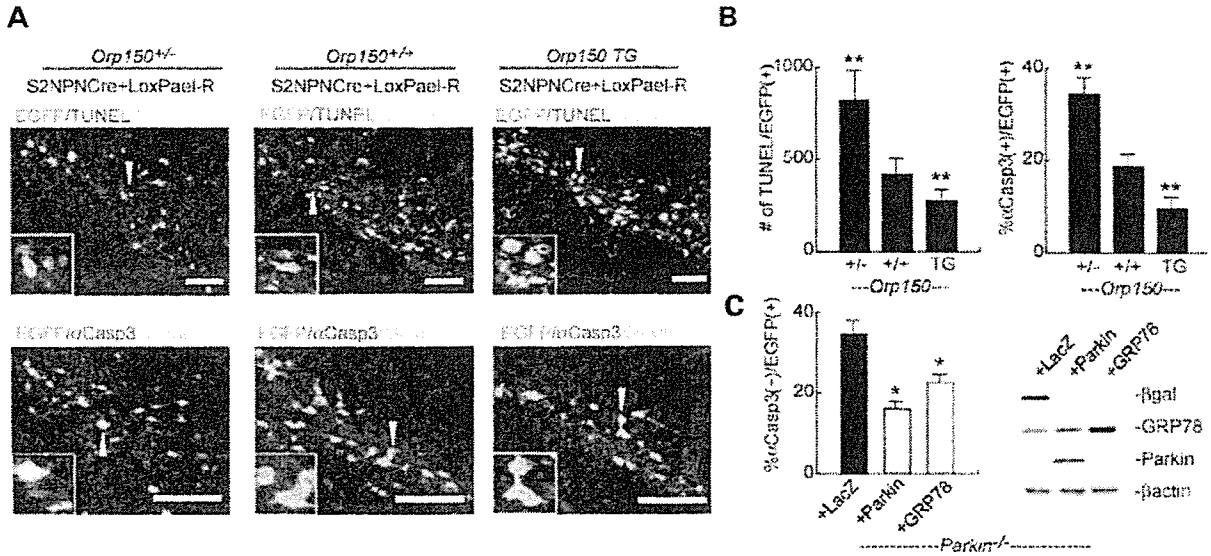

Figure 5. Effect of ORP150, Parkin, and GRP78 on Pael-R-mediated cell death in the SNpc. (**A**) Adenoviral vectors (2 μl), including LoxEGFP (5×10^8 p.f.u.), S2NPNCre (10^9 p.f.u.), and LoxPael-R (10^9 p.f.u.), were injected unilaterally into the striatum of either ORP150$^{+/-}$ (left panels), ORP150$^{-/-}$ (middle panels) or ORP150 transgenic mice (ORP150 TG; right panels) mice. Where indicated, LoxPael-R was replaced with LoxLacZ (10^9 p.f.u.), and the latter mixture was injected on the contralateral side. Brains were then perfusion fixed at 7 (for TUNEL analysis; upper panels) and 5 (for activated caspase-3 staining; αCasp3, lower panels) days after the injection. Images were overlapped with the EGFP signal (green). In each panel, the area indicated by the arrowhead is magnified in a small inset in the lower corner. Note the increase in cells staining positively by TUNEL analysis and for activated caspase-3 antigen in the EGFP positive area. This was most apparent in ORP150$^{+/-}$ mice. Scale bar: 200 μm. All images shown in this figure are representative of six repeated experiments. (**B**) Total number of TUNEL-positive signals (left panel) and the percentage of activated caspase-3 (αCasp3) positive cells in the population of EGFP-positive neurons (right panels) determined in the ipsilateral SNpc. In each case, $n = 6$, and the mean ± SD is shown. ** denotes $P < 0.01$ compared to ORP150$^{+/+}$ (wild type) mice. (**C**) A mixture (total 2 μl) of LoxEGFP (5×10^8 p.f.u.), S2NPNCre (10^9 p.f.u.), LoxPael-R (10^9 p.f.u.), and LoxLacZ (1.5×10^9 p.f.u.) was injected unilaterally into the striatum of parkin$^{-/-}$ mice. On the contralateral side, LoxLacZ was replaced with either AxCMParkin (Parkin; 1.5×10^9 p.f.u.) or AxCAGRP78 (GRP78; 1.5×10^9 p.f.u.). Midbrain sections were stained with anti-activated caspase-3 antibody (5 days later). The percentage of activated caspase-3-positive neurons was determined on the ipsilateral (closed bars) and contralateral sides. In the latter case, data is shown following injection of the vector expressing parkin (gray bars) and GRP78 (open bars) are shown. In each case, $n = 6$, and the mean ± S.D is shown. Midbrain samples collected from parkin$^{-/-}$ mice as described in text were also subjected to Western blot analysis using either anti-β-galactosidase, anti-GRP78, anti-Parkin or anti-β-actin antibody (for an internal control). A typical example of five repeated experiments is shown. * denotes $P < 0.01$ compared to the group injected with the vector expressing LacZ.

the regulation of dopamine levels; increased Pael-R is associated with increased dopamine content in the striatum (Imai, Y. *et al.*, manuscript in preparation). Based on these observations, we reasoned that Pael-R-mediated cell death in the SNpc of *Parkin*$^{-/-}$ mice might be associated with elevated levels of dopamine. Since dopamine has considerable potential toxicity (8,22), we further hypothesized that dopamine-derived metabolites/catabolites might contribute to loss of TH-positive (+) neurons. To address this issue directly, we determined whether suppression of DA synthesis by AMPT, a specific inhibitor of TH (15), would have a neuroprotective effect on TH(+) neurons overexpressing Pael-R in the SNpc of *Parkin*$^{-/-}$ mice. Accidental death of mice occurred in ≈4% of animals within 36 h after the first administration of AMPT. This might be due to the shifts of circadian temperature rhythms (23). The systemic toxicity of AMPT was not observed at later phase. Repeated administration of AMPT over a 7 day period lowered dopamine content of the striatum to ≈30% of that observed in untreated controls (Supplementary Material, Fig. S5). Using this protocol of AMPT treatment, adenoviral vectors were injected into the striatum to increase neuronal Pael-R levels in *Parkin*$^{-/-}$ mice. Compared with *Parkin*$^{-/-}$ mice treated with phosphate-buffered saline (PBS), animals receiving AMPT displayed striking neuroprotection. Inhibition of TH in *Parkin*$^{-/-}$ mice overexpressing Pael-R in the SNpc suppressed the number of TUNEL-positive nuclei and generation of activated caspase-3 epitopes, compared with animals treated with PBS alone (Fig. 6A–C). AMPT treatment was also effective in preventing Pael-R-mediated cell death in the SNpc of *Orp150*$^{+/-}$ mice, compared with animals treated with saline (Fig. 6C), suggesting a toxic effect of DA in ER dysfunction. These data suggest that dopamine enhances neurotoxicity associated with overexpression of Pael-R, especially in the absence of Parkin.

DISCUSSION

Our data indicate that *in vivo* overexpression of Pael-R in neurons of the SNpc results in enhanced ER stress, which, especially in a setting with decreased functional Parkin, targets TH-positive neurons for accentuated cytotoxicity. Whereas expression of a protein as difficult to properly fold as Pael-R has been shown to cause ER stress in a range of cell types *in vitro* (9), we believe that cellular vulnerability in this situation is critically exaggerated in dopaminergic neurons *in vivo* due to the superimposed toxicity of dopamine

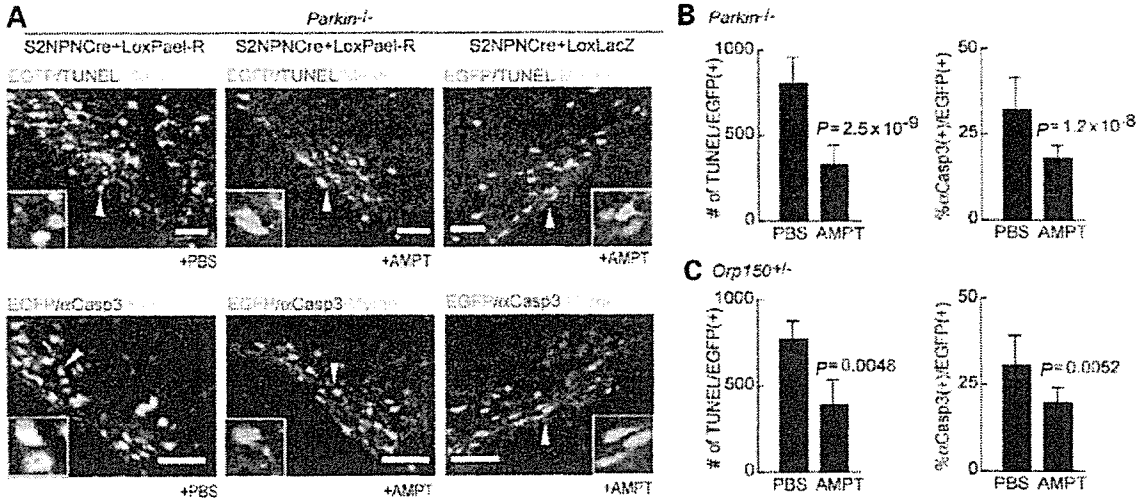

Figure 6. Suppression of neuronal death in the SNpc of mice overexpressing Pael-R by inhibition of dopamine synthetase using AMPT. (**A**) Parkin$^{-/-}$ mice were treated with either PBS or AMPT up to 7 days after unilateral injection of adenoviral vectors, including LoxEGFP (5×10^8 p.f.u.), S2NPNCre (10^9 p.f.u.) and LoxPael-R (10^9 p.f.u.). As a control, the same vectors, with LoxPael-R replaced by LoxLacZ (10^9 p.f.u.), were injected on the contralateral side. Brains were perfusion-fixed at 7 (upper panels; for TUNEL analysis) and 5 (lower panels; staining for activated caspase-3, αCasp3) days after injection of the vectors, and were then subjected to histochemical analysis as described above. The above images were overlapped with EGFP (green). Scale bar: 200 μm. All images shown in this figure are representative of six repetitions of the experimental protocol. In each panel, the area indicated by the arrowhead is magnified in a small inset in the lower corner. Note that TUNEL-positive and activated caspase-3-positive cells were diminished by AMPT treatment (i.e. in the presence of the latter, the area/level of apoptotic cells approximated that observed in controls overexpressing LacZ). (**B,C**) Statistical analysis was performed as described above, in either *Parkin*$^{-/-}$ mice (B) or *Orp150*$^{+/-}$ mice (C). The number of TUNEL-positive signals (left panels), and % of activated caspase-3-positive cells in the population of EGFP-positive neurons (right panels) in the ipsilateral SNpc are shown ($n = 6$; the mean ± SD). *P*-values obtained by Student's t-analysis, are shown in each panel.

(DA) itself. These data also emphasize the potential relevance of parkin targets, such as Pael-R, in addition to the aminoacyl-tRNA synthetase cofactor p38, to neurotoxicity in dopaminergic neurons (24).

The technical approach employed in our experiments, injection of adenovirus under stereotactic guidance into the striatum with selective neuronal expression of gene products, is quite unique. First, such results have been difficult to achieve in the mouse because of anatomic limitations. Though adenovirus vectors are more immunogenic than adenovirus associated virus, they still have greater merits in retrograde transfection (25). We have taken this advantage into our experimental system, to achieve an efficient gene transfer to SNpc, where direct injection of viral vectors will be inapplicable because of anatomical limitations. Second, adenovirus infection predominately affects glia, rather than neurons. Modification of the SCG10 (superior cervical ganglion) promoter by tandem insertion of two neuron-restrictive silencers produced almost 100% expression of transgenes in neuronal cultures, and considerably lower expression in astrocytes (not shown). Coinjection of S2NPNCre with LoxEGFP into the striatum resulted in expression of transgenes in neurons of the mouse SNpc. This approach allowed us to obtain neuron-specific expression of Pael-R enabling study of its effect(s) on neuronal physiology *in vivo*. The proximal result of such Pael-R expression included upregulation of ER chaperones, such as GRP78 and ORP150, whereas the distal result was loss of TH-positive neurons, especially in *Parkin*$^{-/-}$ mice. In contrast, expression of Pael-R had no effect on the constitutively expressed form of HSP70, important for housekeeping functions in the cytoplasm (Fig. 2D).

Several observations are consistent with the importance of ER stress as a mechanism underlying Pael-R-induced cellular toxicity. In previous studies using cultured neuroblastoma cells, Pael-R has been identified as a substrate of Parkin, an E3 ubiquitin ligase (6). Thus, in the absence of Parkin, Pael-R may accumulate since it is not subject to efficient removal. In contrast, no detectable change of Pael-R levels has been reported in SNpc of Parkin null mice (24). Since there is no evidence of progressive neuronal cell death in Parkin null mice, there would appear to be redundant mechanisms able to compensate for loss of Parkin under physiologic conditions. The ability of neurons to withstand ER stress imposed by expression of Pael-R is likely to be dependent on the effectiveness of the ER-stress response; higher levels of Pael-R would require a facile ER-stress response (i.e. adequate or increased levels of parkin, ORP150, GRP78 etc), whereas diminished levels of ORP150 or GRP78 would render neurons vulnerable to toxicity because of a compromised stress response. These predictions have been borne out by our experimental results. Therefore, the possible toxicity of Pael-R cannot be completely ignored, especially in pathological conditions. Increasing expression of GRP78 had a protective effect in *Parkin*$^{-/-}$ mice overexpressing Pael-R. Furthermore, expression of ORP150, an important factor modulating ER stress even in the presence of Parkin, modulated the toxicity of Pael-R for dopaminergic neurons; increased levels of ORP150 in transgenic mice were neuroprotective, whereas diminished levels in ORP150 in *Orp150*$^{+/-}$ mice resulted in enhanced cell death (i.e. increased TUNEL staining and immunoreactivity for activated caspase-3 in the SNpc).

Our experimental system produced Pael-R overexpression and subsequent cell death in the SNpc of mouse, whereas no apparent cell death occurred either in the striatum or in the motor cortex (Supplementary Material, Fig. S2C). Furthermore, we observed a neuroprotective effect of a TH inhibitor in the SNpc of mouse, suggesting that DA also contributes to Pael-R-induced cell death of dopaminergic neurons. Consistent with these results in our mouse models, studies in transgenic flies overexpressing Pael-R in most of neuronal populations also showed selective loss of dopaminergic neurons, though the mechanism of cellular degeneration is not fully understood (10). One plausible explanation for focusing toxicity on dopaminergic neurons is the oxidative stress caused by the presence of DA and its derivatives (1). Another possibility that DA might compromise the survival of dopaminergic neurons is a chemical inactivation of cellular proteins by addition of DA to sulfhydryl group of proteins. Recently, it has been reported that dopamine covalently modifies Parkin, a protein rich in sulfhydryl group, in dopaminergic cells, leading to increased Parkin insolubility and inactivation of its E3 function (22). Vulnerability of Parkin to modification by DA further impairs degradation of Pael-R. Thus, even in sporadic PD, DA might interfere in the degradation of certain proteins, such as Pael-R, by the inactivation of Parkin. Collectively, these data propose a model in which a combination of ER stress and DA-related stress plays an important role in degeneration of dopaminergic neurons in sporadic PD as well as PD caused by *parkin* mutations.

MATERIALS AND METHODS

Targeted disruption of the mouse parkin gene

Parkin$^{-/-}$ mice were generated using standard gene targeting techniques (26). A targeting vector was constructed with a 15.7 kb genomic DNA fragment containing exon 3 of the parkin gene (Supplementary Material, Fig. S1). The region containing exon 3 was replaced with a Floxed pgk-neo cassette. A DT-ApA cassette was flanked at the 5′-end of the homologous arm for negative selection (27). The linearized targeting vector was transfected into E14 (129sv) ES cells. Positive clones were selected by Southern blotting, and then injected into C57Bl/6J (B6) blastocysts. Offspring harboring the targeted allele were generated by crossing chimeric mice with B6 mice. Results of such crosses were confirmed by Southern analysis.

Reverse transcription–polymerase chain reaction analysis of parkin null mice

Total RNA was extracted from whole brain tissue using Isogen (Nippon gene). RT reactions containing 1 μg of total RNA were performed using the SuperScript II First-Strand Synthesis System for RT–PCR (Invitrogen). The resulting cDNA was added to PCR reactions containing 1 unit of Ex *Taq* DNA Polymerase (Takara) for 35 PCR cycles. PCR products were separated on a 1% agarose gel. Primers were as follows: RT primer, 5′-agt ttc cct tga ggt tgt gc; Primer A, 5′-cgt agg tcc ttc tcg acc; Primer B, 5′-ttg agg ttg tgc gtc cag g; Primer C, 5′-acc tca gag ggc tcc ata tg; and, Primer D, 5′-ctc tct cta cac gtc aaa cca gtg.

Construction of adenoviral vectors

Modified SCG10 (S2NP10) promoter [2 kb (28)] and mouse GFAP promoter region (2.5 kb: kindly provided by Dr Ikenaka, National Institute for Physiological Science) were cloned into pAxAwNCre (kindly provided by Dr Saito, Tokyo University), a promoter-less cosmid vector for preparing cell type-specific Cre-recombinase expressing adenovirus (Fig. 2A; AxS2NPNCre and AxGFAPNCre). Human Pael-R (9) was cloned into pAxCALNLw (Takara Bio Inc., Shiga, Japan) in order to control Pael-R expression using Cre recombinase (AxLNLPael-R). The Pael-R gene is silenced because of the presence of the staffer of the neo-resistant gene, and is activated by Cre-mediated excisional deletion of the stuffer when a sufficient amount of Cre recombinase is expressed (Fig. 3). To prepare an adenoviral vector of parkin (AxCMParkin), the human parkin gene was cloned into pAxCMwt. Recombinant adenovirus was generating using the COS-terminal protein complex (TPC) method and the Takara adenovirus expression kit (Takara Bio Inc.). AxLNLNZ (Takara Bio Inc.), which overexpresses LacZ with a nuclear localization signal mediated by Cre recombinase, was used for control experiments. Cre-mediated EGFP-expressing adenovirus, AxLNLEGFP, was kindly provided by Dr Okado (Tokyo Metropolitan Institute of Neuroscience). An adenoviral vector for overexpression of GRP78/Bip (AxCAGRP78) was generously provided by Drs S. Tanaka and T. Koike [(29) Graduate School of Science, Hokkaido University]. Each adenovirus was amplified in HEK293 cells and purified using VIRAPREP Adenovirus Purification Kit (Virapur LLC., San Diego, CA, USA). Viral titers were determined by a plaque-forming assay in HEK293 cells.

Western blotting

Levels of Pael-R in tissue extracts were determined by Western blotting as described (9). Mouse brain was quickly removed and placed on a cold plate. Brain slices (200 μm) were obtained at −3.5 mM from the Bregma on a vibratome. Substantia nigra was then carefully removed under guidance of a stereoscopic microscope according to the mouse brain atlas (Paxinos and Franklin, Academic Press, 1997, San Diego) using the cerebral peduncle and medial lemniscus as landmarks. Tissue extracts were prepared from SNpc in PBS containing NP-40 (1%). Proteins were separated by SDS-PAGE, and transferred to PVDF. PVDF was then incubated with antibody to either human Pael-R or ß-actin, the latter as an internal control (1000 × dilution, Sigma, St Louis, MO, USA). Levels of chaperones in tissue extracts were determined by Western blotting, as described (30). PVDF was incubated with either anti-human ORP150 antibody (1 μg/ml), anti-GRP78 monoclonal antibody (Stressgen, Canada; 0.2 μg/ml), or anti-HSP73 antibody (0.1 μg/ml; Stressgen). Where indicated, either anti-β-galactosideas antibody (1000 × dilution, Sigma) or anti-Parkin antibody (1000 × dilution, Cell Signaling Technologies Inc.) was

used to access the level of these proteins. Images were further subjected to densitometric analysis using NIH image software.

Injection of adenoviral vectors into the striatum and treatment of animals

Animals were housed and treated according to institutional and national guidelines. Mice were stereotactically positioned under deep anesthesia, and the indicated combination of adenovirus vectors was injected unilaterally (a different combination, including a LacZ control, was injected on the contralateral side) into the striatum at six points (AP/ML/DV/ = 0.8/1.2/−2.5, 0.8/1.2/−3.2, 0.8/1.7/−2.5, 0.8/1.7/−3.2, 0.8/2.2/−2.5 and 0.8/2.2/−3.2; units are mm), followed by free access to food and water. Retrograde passage and infection of adenoviruses was confirmed 5–12 days after the injection by detection of a green fluorescent signal in the SNpc by fluorescence microscopy. Where indicated, animals were pretreated with α-methyl-DL-Tyrosine (AMPT) to suppress DA synthesis. AMPT-HCl (150 mg/kg, Sigma) was intra-peritoneally administrated twice per day for 5 days before injection of adenoviral vectors, as well as after the latter and until the day of sacrifice.

Assessment of neuronal death *in vivo*

At the indicated time points, animals were perfused with 4% paraformaldehyde under deep anesthesia, the brain was excised and coronal brain sections (14 μm) were cut on a cryostat. Sections were processed for cresyl violet staining or immunohistochemistry using either mouse anti-tyrosine hydroxylase antibody (TH; 1 μg/ml, Sigma), rabbit anti-human ORP 150 antibody [5 μg/ml (30)], rabbit anti-activated caspase-3 antibody(0.1 μg/ml, Genzyme/Teche), rabbit anti-Pael-R antibody [10 μg/ml, (9)] or goat anti-GFAP antibody (4 μg/ml. Santa Cruz Biotechnology, Santa Cruz, CA). Sections were also subjected to TUNEL staining using a commercially available kit (ApopTag, Intergen, Purchase, NY). To evaluate neuronal death in the SNpc, either Nissl or EGFP positive cells were counted in each coronal slice obtained at five different levels (−3.16, −3.28, −3.40, −3.52 and −3.64 mM from the Bregma), as described (31) by acquiring digital images using a CCD camera (Nikon, Coolscope). Cell death was semi-quantitatively assessed by counting TUNEL-positive cells/nuclei in the EGFP-positive area, and evaluating the percentage of activated caspase-3-positive cells in the population of EGFP-positive cells. Sections were analyzed using a laser scanning confocal microscope system (Leica, TCS SP2). In each case, two observers without knowledge of the experimental protocol evaluated sections and experiments were repeated at least three times.

DA content in the striatum was measured in the SNpc as described (32). In brief, striatal tissue was homogenized in solution H (0.4 M $HClO_4$ containing 4 mM $Na_2S_2O_5$, 4 mM diethylenetriaminepentaacetic acid, and 5 mM 1,4-dithiothreitol). Crude tissue lysate was separated on a C-18 reversed-phase column (MCM HPLC, 4.6 mM × 15 cm, 5 ml, ESA, Chelmsford, MA, USA), followed by electrochemical detection (Coulochem III, ESA).

Statistical analysis

Data shown represent the mean ± SD Multiple group comparisons were performed by one-way ANOVA, followed by Newman-Kuels test as a *post hoc* analysis. Comparison between two groups was analyzed by two-tailed Student's *t*-test.

SUPPLEMENTARY MATERIAL

Supplementary Material is available at HMG Online.

ACKNOWLEDGEMENTS

We thank Dr Martin Hooper (Western General Hospital, Edinburgh) for generous contribution of E14 cell line, and Drs Yumi Onodera, Yoshikazu Saito, Hitomi Suzuki (RIKEN, Wako, Japan) for technical assistance for establishing chimera mice. The authors also appreciate the generous gifts of AxCALNLEGFP, GAG promoter and Ax1CAGRP78 from Drs Haruo Okado (Tokyo Metropolitan Institute for Neuroscience), Jun-Ichi Miyazaki (Osaka University Medical School), and Shuuitsu Tanaka and Tetsuro Koike (Hokkaido University), respectively. This work was partially supported by the Ministry of Education, Science, Sports and Culture, a Grant-in-Aid for Scientific Research on Priority Areas—Advanced Brain Science Project—#15016120 to R.T., for Scientific Research (A) #14207032 to R.T., and for Young Scientists (A) #15680011 to Y.I. and a grant from the Special Postdoctoral Researcher Program of RIKEN to Y.I.

Conflict of Interest statement. None declared.

REFERENCES

1. Blum, D., Torch, S., Lambeng, N., Nissou, M., Benabid, A.L., Sadoul, R. and Verna, J.M. (1999) Molecular pathways involved in the neurotoxicity of 6-OHDA, dopamine and MPTP: contribution to the apoptotic theory in Parkinson's disease. *Trends. Biochem. Sci.*, **24**, 135–172.
2. Kitada, T., Asakawa, S., Hattori, N., Matsumine, H., Yamamura, Y., Minoshima, S., Yokochi, M., Mizuno, Y. and Shimizu, N. (1998) Mutations in the parkin gene cause autosomal recessive juvenile parkinsonism. *Nature*, **392**, 605–608.
3. Morett, E. and Bork, P. (1999) A novel transactivation domain in parkin. *Trends. Biochem. Sci.*, **24**, 229–231.
4. Jackson, P.K., Eldridge, A.G., Freed, E., Furstenthal, L., Hsu, J.Y., Kaiser, B.K. and Reimann, J.D. (2000) The lore of the RINGs: substrate recognition and catalysis by ubiquitin ligases. *Trends. Cell. Biol.*, **10**, 429–439.
5. Takahashi, R., Imai, Y., Hattori, N. and Mizuno, Y. (2003) Parkin and endoplasmic reticulum stress. *Ann. N.Y. Acad. Sci.*, **991**, 101–106.
6. Imai, Y., Soda, M. and Takahashi, R. (2000) Parkin suppresses unfolded protein stress-induced cell death through its E3 ubiquitin-protein ligase activity. *J. Biol. Chem.*, **275**, 35661–36664.
7. Shimura, H., Hattori, N., Kubo, S., Mizuno, Y., Asakawa, S., Minoshima, S., Shimizu, N., Iwai, K., Chiba, T., Tanaka, K. and Suzuki, T. (2000) Familial Parkinson disease gene product, parkin, is a ubiquitin-protein ligase. *Nat. Genet.*, **25**, 302–305.
8. Tanaka, K., Suzuki, T., Hattori, N. and Mizuno, Y. (2004) Ubiquitin, proteasome and parkin. *Biochim. Biophys. Acta.*, **29**, 235–247.
9. Imai, Y., Soda, M., Inoue, H., Hattori, N., Mizuno, Y. and Takahashi, R. (2001) An unfolded putative transmembrane polypeptide, which can lead to endoplasmic reticulum stress, is a substrate of Parkin. *Cell.*, **105**, 891–902.

10. Yang, Y., Nishimura, I., Imai, Y., Takahashi, R. and Lu, B. (2003) Parkin suppresses dopaminergic neuron-selective neurotoxicity induced by Pael-R in drosophila. *Neuron*, **27**, 911–924.
11. Tamatani, M., Matsuyama, T., Yamaguchi, A., Mitsuda, N., Tsukamoto, Y., Taniguchi, T., Che, Y.H., Ozawa, K., Hori, O., Nishimura, H. *et al.* (2001) ORP150 protects against hypoxia/ischemia-induced neuronal death. *Nat. Med.*, **7**, 317–323.
12. Miyazaki, M., Ozawa, K., Hori, O., Kitao, Y., Matsushita, K., Ogawa, S. and Matsuyama, T. (2002) Expression of ORP150 (150 kDa oxygen regulated protein) in the hippocampus suppresses delayed neuronal cell death. *J. Cereb. Blood Flow Metab.*, **22**, 979–987.
13. Kitao, Y., Ozawa, K., Miyazaki, M., Tamatani, M., Kobayashi, T., Yanagi, H., Okabe, M., Ikawa, M., Yamashima, T., Tohyama, M. *et al.* (2001) Expression of 150 kDa Oxygen Regulated Protein (ORP150), a molecular chaperone in the endoplasmic reticulum, rescues hippocampal neurons from glutamate toxicity. *J. Clin. Invest.*, **108**, 1439–1450.
14. Kitao, Y., Hashimoto, K., Matsuyama, T., Iso, H., Tamatani, T., Hori, O., Stern, D.M., Kano, M., Ozawa, K. and Ogawa, S. (2004) ORP150/HSP12A regulates Purkinje cell survival: a role for endoplasmic reticulum stress in cerebellar development. *J Neurosci.*, **24**, 1486–1496.
15. Dong, Z., Ferger, B., Paterna, J.C., Vogel, D., Furler, S., Osinde, M., Feldon, J. and Bueler, H. (2003) Dopamine-dependent neurodegeneration in rats induced by viral vector-mediated overexpression of the parkin target protein, CDCrel-1. *Proc. Natl Acad. Sci. U.S.A.*, **100**, 12438–12443.
16. Kanegae, Y., Lee, G., Sato, Y., Tanaka, M., Nakai, M., Sakaki, T., Sugano, S. and Saito, I. (1995) Efficient gene activation in mammalian cells by using recombinant adenovirus expressing site-specific Cre recombinase. *Nucleic Acids Res.*, **23**, 3816–3821.
17. Bando, Y., Ogawa, S., Yamaguchi, A., Kuwabara, K., Ozawa, K., Hori, O., Yanagi, H., Tamatani, M. and Tohyama, M. (2000) The 150 kDa Oxygen Regulated Protein (ORP150) functions as a novel molecular chaperone in the protein transport of the MDCK cells. *Am. J. Physiol. (Cell Physiol.)*, **278**, C1172–C1182.
18. Itier, J.M., Ibanez, P., Mena, M.A., Abbas, N., Cohen-Salmon, C., Bohme, G.A., Laville, M., Pratt, J., Corti, O., Pradier, L. *et al.* (2003) Parkin gene inactivation alters behaviour and dopamine neurotransmission in the mouse. *Hum. Mol. Genet.*, **12**, 2277–2291.
19. Goldberg, M.S., Fleming, S.M., Palacino, J.J., Cepeda, C., Lam, H.A., Bhatnagar, A., Meloni, E.G., Wu, N., Ackerson, L.C., Klapstein, G.J. *et al.* (2003) Parkin-deficient mice exhibit nigrostriatal deficits but not loss of dopaminergic neurons. *J. Biol. Chem*, **278**, 43628–43635.
20. Selimi, F., Doughty, M., Delhaye-Bouchaud, N. and Mariani, J. (2000) Target-related and intrinsic neuronal death in lurcher mutant mice are both mediated by caspaea-3 actvation. *J. Neurosci.*, **20**, 992–1000.
21. Bando, Y., Tsukamoto, Y., Katayama, T., Ozawa, K., Kitao, Y., Hori, O., Stern, D.M., Yamauchi, A. and Ogawa, S. (2004) ORP150/HSP12A protects renal tubular epithelium from ischemia-induced cell death. *FASEB J.*, **18**, 1401–1403.
22. Lavoie, M.J., Ostaszewski, B.L., Weihofen, A., Schlossmacher, M.G. and Selkoe, D.J. (2005) Dopamine covalently modifies and functionally inactivates parkin. *Nat. Med.*, **11**, 1214–1221.
23. Cahill, A.L. and Ehret, C.F. (1982) Alpha-methyl-p-tyrosine shifts circadian temperature rhythms. *Am. J. Physiol.*, **243**, R218–R222.
24. Ko, H.S., vonCoelln, R., Sriram, S.R., Kim, S.W., Chung, K.K., Pletnikova, O., Troncoso, J., Johnson, B., Saffary, R., Goh, E.L. *et al.* (2005) Accumulation of the authentic parkin substrate aminoacyl-tRNA synthetase cofactor, p38/JTV-1, leads to catecholaminergic cell death. *J. Neurosci.*, **25**, 7968–7978.
25. Barkats, M., Bilang-Bleuel, A., Buc-Caron, M.H., Castel-Barthe, M.N., Corti, O., Finiels, F., Horellou, P., Revah, F., Sabate, O. and Mallet, J. (1998) Adenovirus in the brain: recent advances of gene therapy for neurodegenerative diseases. *Prog. Neurobiol.*, **55**, 333–341.
26. Gomi, H., Yokoyama, T., Fujimoto, K., Ikeda, T., Katoh, A., Itoh, T. and Itohara, S. (1995) Mice devoid of the glial fibrillary acidic protein develop normally and are susceptible to scrapie prions. *Neuron*, **14**, 29–41.
27. Yanagawa, Y., Kobayashi, T., Ohnishi, M., Kobayashi, T., Tamura, S., Tsuzuki, T., Sanbo, M., Yagi, T., Tashiro, F. and Miyazaki, J. (1999) Enrichment and efficient screening of ES cells containing a targeted mutation: the use of DT-A gene with the polyadenylation signal as a negative selection maker. *Transgenic Res.*, **8**, 215–221.
28. Namikawa, K., Murakami, K., Okamoto, T., Okado, H. and Kiyama, H. (2006) A newly modified SCG10 promoter and Cre/loxP-mediated gene amplification system achieve highly specific neuronal expression in animal brains. *Gene Ther.*, **13**, 1244–1250.
29. Satoh, T., Furuta, K., Tomokiyo, K., Nakatsuka, D., Tanikawa, M., Nakanishi, M., Miura, M., Tanaka, S., Koike, T., Hatanaka, H. *et al.* (2000) Facilitatory roles of novel compounds designed from cyclopentenone prostaglandins on neurite outgrowth-promoting activities of nerve growth factor. *J. Neurochem.*, **75**, 1092–1102.
30. Kuwabara, K., Matsumoto, M., Ikeda, J., Hori, O., Ogawa, S., Maeda, Y., Kitagawa, K., Imuta, N., Kinoshita, K., Stern, D. *et al.* (1996) Purufucation and characterization of a novel stress protein, the 150 kDa oxygen regulated protein (ORP150), from cultured rat astrocytes, and its expression in ischemic mouse brain. *J. Biol. Chem.*, **279**, 5025–5032.
31. Kuhn, K., Wellen, J., Link, N., Maskri, L., Lubbert, H. and Stichel, C.C. (2003) The mouse MPTP model: gene expression changes in dopaminergic neurons. *Eur. J. Neurosci.*, **17**, 1–12.
32. Itoh, S., Katsuura, G. and Takashima, A. (1988) Effect of vasoactive intestinal peptide on dopaminergic system in the rat brain. *Peptides*, **9**, 315–317.

The EMBO Journal (2006) 25, 211–221 | © 2006 European Molecular Biology Organization | All Rights Reserved 0261-4189/06
www.embojournal.org

THE EMBO JOURNAL

14-3-3η is a novel regulator of parkin ubiquitin ligase

Shigeto Sato[1,2], Tomoki Chiba[2], Eri Sakata[3], Koichi Kato[3], Yoshikuni Mizuno[1], Nobutaka Hattori[1] and Keiji Tanaka[2,*]

[1]Department of Neurology, Juntendo University School of Medicine, Bunkyo, Tokyo, Japan, [2]Tokyo Metropolitan Institute of Medical Science, Bunkyo-ku, Tokyo, Japan and [3]Department of Structural Biology and Biomolecular Engineering, Graduate School of Pharmaceutical Sciences, Nagoya City University, Mizuho-ku, Nagoya, Japan

Mutation of the *parkin* gene, which encodes an E3 ubiquitin-protein ligase, is the major cause of autosomal recessive juvenile parkinsonism (ARJP). Although various substrates for parkin have been identified, the mechanisms that regulate the ubiquitin ligase activity of parkin are poorly understood. Here we report that 14-3-3η, a chaperone-like protein present abundantly in neurons, could bind to parkin and negatively regulate its ubiquitin ligase activity. Furthermore, 14-3-3η could bind to the linker region of parkin but not parkin with ARJP-causing R42P, K161N, and T240R mutations. Intriguingly, α-synuclein (α-SN), another familial Parkinson's disease (PD) gene product, abrogated the 14-3-3η-induced suppression of parkin activity. α-SN could bind tightly to 14-3-3η and consequently sequester it from the parkin–14-3-3η complex. PD-causing A30P and A53T mutants of α-SN could not bind 14-3-3η, and failed to activate parkin. Our findings indicate that 14-3-3η is a regulator that functionally links parkin and α-SN. The α-SN-positive and 14-3-3η-negative control of parkin activity sheds new light on the pathophysiological roles of parkin.

The EMBO Journal (2006) **25**, 211–221. doi:10.1038/sj.emboj.7600774; Published online 11 August 2005
Subject Categories: proteins; molecular biology of disease
Keywords: α-synuclein; 14-3-3η; parkin; Parkinson's disease; ubiquitin ligase

Introduction

In the last decade, people working in the field of Parkinson's disease (PD) witnessed a tremendous progress in uncovering the mechanisms of PD, and several familial PD genes were discovered in succession (Vila and Przedborski, 2004). Of these hereditary PD genes, *parkin* (*PARK2*), the causative gene of autosomal recessive juvenile parkinsonism (ARJP), is of a special interest because it encodes a ubiquitin ligase, a critical component of the pathway that covalently attaches ubiquitin to specific proteins with a polymerization step to form a degradation signal (Shimura *et al*, 2000). Indeed, parkin catalyzes the addition of ubiquitin to target proteins prior to their destruction via the proteasome, suggesting that the misregulation of proteasomal degradation of parkin substrate(s) is deleterious to dopaminergic neurons (Dawson and Dawson, 2003; Bossy-Wetzel *et al*, 2004; Kahle and Haass, 2004). Consequently, impaired protein clearance can induce dopaminergic cell death, supporting the concept that defects in the ubiquitin–proteasome system may underlie nigral degeneration in ARJP and perhaps sporadic forms of PD (McNaught and Olanow, 2003). On the other hand, it was recently reported that parkin also catalyzes the formation of the K63-linked polyubiquitylation chain, independent of proteasomal destruction, in which the K48-linked polyubiquitylation chain is necessary (Doss-Pepe *et al*, 2005; Lim *et al*, 2005). Thus, it is plausible that parkin shares two roles as an E3 ligase; that is, one linking to and the other independent of the proteasome.

Among the products of major familial PD genes (Vila and Przedborski, 2004), α-synuclein (α-SN) is a product of familial PD gene (*PARK1*) identified as a presynaptic protein of unknown function. α-SN is considered in the molecular mechanisms of PD mainly because it is one of the major components of the cytoplasmic Lewy body (LB) inclusion present in the remaining nigral dopaminergic neurons of PD patients, which is the pathological hallmark of sporadic and some familial PDs (Forno, 1996). Although various studies have been conducted on α-SN (Dawson and Dawson, 2003; Bossy-Wetzel *et al*, 2004; Kahle and Haass, 2004), its pathophysiological role(s) and the interplay between α-SN and parkin are largely unknown.

To date, little is known about the role of parkin as a ubiquitin E3 ligase with respect to the underlying molecular mechanism(s) of ARJP or PD. Here we report for the first time that 14-3-3η, a member of the 14-3-3 family (β/α, γ, ε, η, ζ/δ, σ, and τ/θ) (Berg *et al*, 2003; Bridges and Moorhead, 2004; Mackintosh, 2004) identified in LB (Kawamoto *et al*, 2002; Ubl *et al*, 2002), binds primarily to the linker region of parkin and functions as a novel negative regulator of parkin. We also show that α-SN relieves parkin activity suppressed by 14-3-3η, indicating that 14-3-3η is a novel molecule handling both parkin and α-SN, and that functionally links the two familial PD gene products.

Results

Parkin specifically interacts with 14-3-3η but not with other 14-3-3 isoforms

We first examined the physical association of parkin with 14-3-3 isoforms, which are abundantly expressed in the brain (Martin *et al*, 1994; Baxter *et al*, 2002). Parkin was immunoprecipitated from mouse brain extracts, and the presence of 14-3-3 was analyzed by Western blotting (Figure 1A). 14-3-3 was clearly detected in the parkin immunoprecipitant, but not in those of control IgG or parkin antibody preabsorbed

*Corresponding author. Department of Molecular Oncology, The Tokyo Metropolitan Institute of Medical Science, 3-18-22 Honkomagome, Bunkyo-ku, Tokyo 113-8613, Japan. Tel./Fax: +81 3 3823 2237; E-mail: tanakak@rinshoken.or.jp

Received: 24 January 2005; accepted: 15 July 2005; published online: 11 August 2005

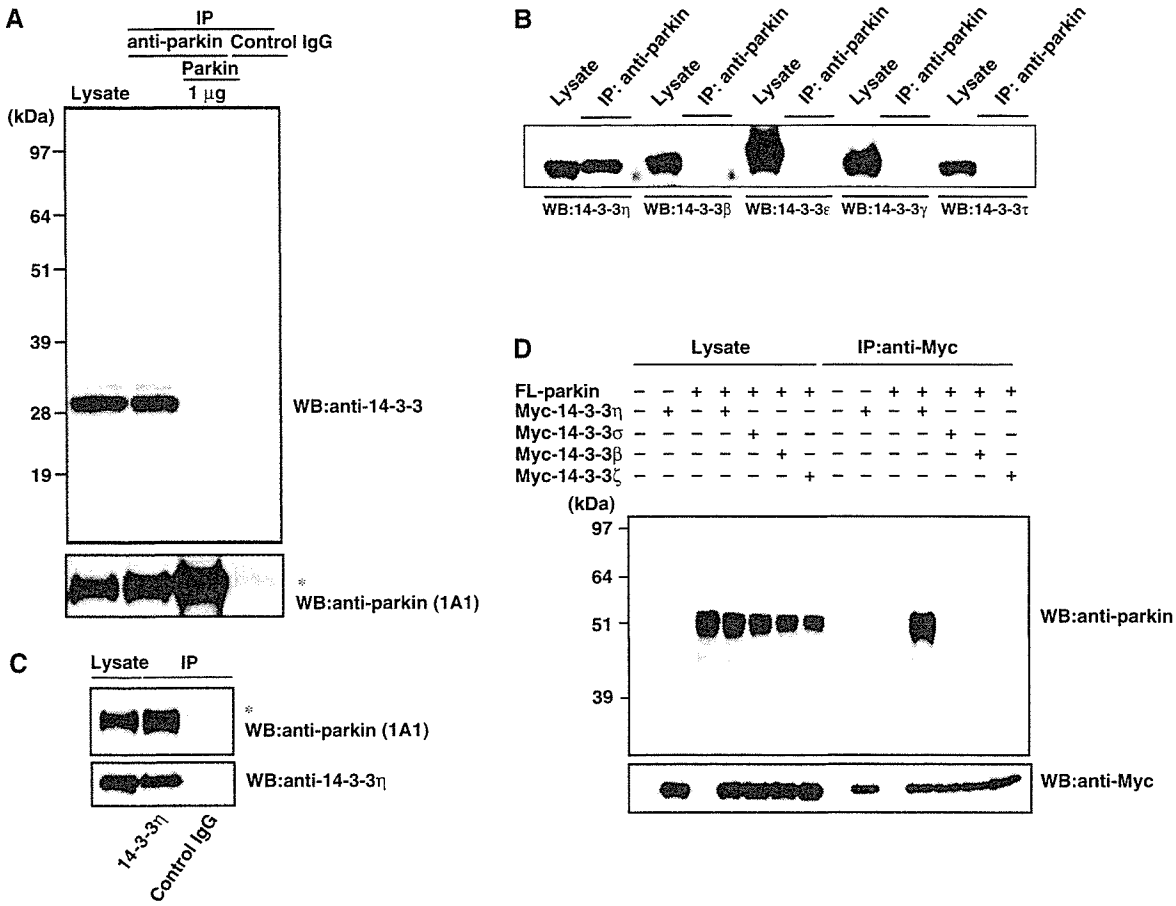

Figure 1 Physical interaction between parkin and 14-3-3η. (**A**) Immunoprecipitation by anti-parkin antibody in the mouse brain. Mouse brain lysates were prepared and treated with anti-parkin or control IgG as described in Materials and methods. The resulting immunoprecipitates were subjected to SDS–PAGE, followed by Western blotting with anti-14-3-3 and parkin (1A1) antibodies. In all, 1 μg of recombinant parkin was pretreated with anti-parkin prior to immunoprecipitation. Left lane: the brain lysate (1.5% input). Asterisk denotes an IgG heavy chain. (**B**) Specificity analysis of 14-3-3 species. The immunoprecipitation with anti-parkin and subsequent SDS–PAGE were carried out as in (A). Western blotting was conducted with antibodies against various 14-3-3 isoforms as indicated for lysates and anti-parkin immunoprecipitates. (**C**) Immunoprecipitation by anti-14-3-3η antibody. After immunoprecipitation with anti-14-3-3η or control IgG of the brain lysate, the immunoprecipitates were analyzed by Western blotting with anti-parkin (1A1) and 14-3-3η antibodies, similar to (A). Left lane: the brain lysate (1.5% input). Asterisk denotes an IgG heavy chain. (**D**) Interaction between parkin and 14-3-3η in HEK293 cells. FL-parkin (5 μg), Myc-14-3-3η, σ, β, or ζ (2 μg) plasmids were transfected as indicated into HEK293 cells. After 48 h, the cell lysate was prepared and used for immunoprecipitation with anti-Myc antibody. The immunoprecipitates and the lysate (7.5% input) were analyzed by Western blotting with anti-parkin and Myc antibodies, as in (A).

with recombinant parkin protein (1 μg). Intriguingly, two 14-3-3 signals were evident: a faint band and a strongly stained band, indicating that the 14-3-3 may form homo- and/or hetero-dimers. Subsequently, we determined the type(s) of 14-3-3 species that interacts with parkin in the mouse brain in more detail. In the parkin immunoprecipitant, 14-3-3η, but not other 14-3-3 isoforms examined, that is, β, γ, ε, and τ, was detected (Figure 1B). In the next step, we examined whether parkin is coimmunoprecipitated with anti-14-3-3η antibody and found parkin in the 14-3-3η immunoprecipitant (Figure 1C). These reciprocal immunoprecipitation experiments revealed that parkin is associated with 14-3-3η in the mouse brain.

To confirm the specific interaction of parkin with 14-3-3η, Myc-tagged 14-3-3η, σ, β, or ζ was cotransfected with FLAG (FL)-parkin into HEK293 cells, and their interactions were tested. FL-parkin was detected in the immunoprecipitant of Myc-14-3-3η, but not those of Myc-14-3-3σ, β, and ζ (Figure 1D). Taken together with the results of Figure 1B, our data indicate that parkin mainly interacts with 14-3-3η.

Parkin domain interacts with 14-3-3η

We next investigated the region of parkin necessary for interaction with 14-3-3η. Structurally, parkin is characterized by the presence of the N-terminal ubiquitin-like domain (UBL) (which is highly homologous to ubiquitin), the C-terminal RING box, consisting of two RING finger motifs, RING1 and RING2, flanked by one IBR (in between RING finger) motif, and a linker region, which connects these N- and C-terminal regions (Shimura *et al*, 2000). In these experiments, various deletion mutants of FL-tagged parkin were expressed in HEK293 cells and immunoprecipitated by FL-antibody beads (Figure 2A). FL-parkin or its derivatives on the beads were further incubated with cell lysates that expressed Myc-14-3-3η, and then the amounts of Myc-14-3-3η bound to the beads were determined (Figure 2B).

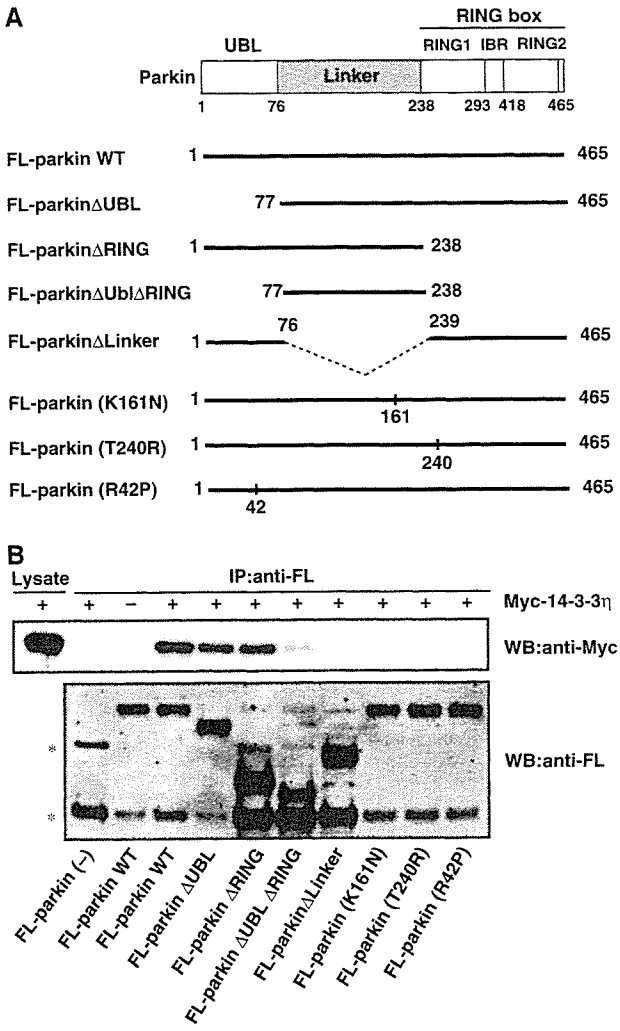

Figure 2 Domain analysis of the parkin region that interacts with 14-3-3η. (**A**) Schematic representation of WT parkin and its deletion- and disease-related missense mutants. See text for the domain structures of parkin and mutants. The dotted line denotes the deleted region. (**B**) Interaction between 14-3-3η and parkin mutants. FL-parkin (2 μg) or its mutant (10 μg) plasmids were transfected into HEK293 cells, as described in Figure 1D. The cell lysates (200–600 μl) were immunoprecipitated with anti-FL-antibody beads. Note that various amounts of the lysates were used to adjust roughly the levels of expressed parkin mutants. The resulting immunoprecipitates were mixed with other cell lysates (200 μl) prepared from cells that had been transfected with Myc-14-3-3η plasmid (2 μg) and incubated for 6 h at 4°C. Then, the extensively washed immunoprecipitates and cell lysate (7.5% input) were analyzed by Western blotting with anti-Myc and FL antibodies. Asterisks denote nonspecific bands.

The full-length parkin could bind 14-3-3η. Deletion of either UBL or RING-box domain reduced the binding compared to the full-length parkin, although these deletion mutants retained the ability to bind to 14-3-3η. Furthermore, mutants with combined deletions of the UBL and RING-box domains, that is, the linker region, could also bind 14-3-3η to a lesser extent. Conversely, deletion of the linker region resulted in the loss of ability to bind 14-3-3η. Taken together, it is concluded that the linker region is necessary for the interaction between parkin and 14-3-3η, although the UBL and RING-box domains may enhance the binding affinity.

Interestingly, the ARJP disease-causing missense mutation within the linker region, that is, parkin(K161N), in which the Lys residue at position 161 was replaced by Asn residue, showed complete loss of binding to 14-3-3η, confirming the importance of the linker region in the interaction between 14-3-3η and parkin. Unexpectedly, other disease-causing missense mutations of the UBL region, parkin(R42P), and the RING1 region, parkin(T240R), also showed complete loss of interaction with 14-3-3η (Figure 2). Thus, although the UBL and RING-box domains are not primarily required for the binding, both R42P and T240R mutations in the UBL and RING-box domains, respectively, deleteriously affect the neighboring linker domain. Alternatively, since 14-3-3 is known to form a homo- or hetero-dimer, and thus has two binding sites (Aitken *et al*, 2002), it is plausible that 14-3-3η interacts with two distinct regions of parkin, one major site of which is the linker region.

Effect of suppression of 14-3-3η on parkin E3 activity

We next investigated the role of parkin–14-3-3η binding on parkin activity. At first, we tested its effect on the ubiquitin ligase activity of parkin. We incubated recombinant His-parkin with ubiquitin, E1, and E2 (UbcH7) *in vitro*. Under this condition, His-parkin appeared as a smear band, which likely reflects self-ubiquitylation (Figure 3A). Addition of recombinant GST-14-3-3η (Figure 3A, left panel) or untagged 14-3-3η (Figure 3A, right panel) to the reaction reduced the smear of His-parkin, and such reduction was proportionate to the added amount of GST-14-3-3η or 14-3-3η and resulted in the recovery of His-parkin of intact size. In addition, we found that 14-3-3η had no effect on the ubiquitylating activity of phosphorylated IκBα by a fully *in vitro* reconstituted system, containing E1, E2 (Ubc4), and E3 (the $SCF^{\beta TrCP}$ complex; Kawakami *et al*, 2001), indicating that 14-3-3η does not interfere with ubiquitylating reactions in general (data not shown). These results strongly suggest that 14-3-3η suppresses the intrinsic self-ubiquitylation activity of parkin.

We next tested whether 14-3-3η also affects the ubiquitylation activity of parkin in HEK293 cells. First, we examined the self-ubiquitylation of parkin, whose activity was observed by cotransfections of HA-ubiquitin and FL-parkin. Myc-14-3-3η almost completely suppressed the self-ubiquitylation activity of parkin, while Myc-14-3-3σ, β, and ζ had no inhibitory effect (Figure 3B), indicating the specific role of 14-3-3η for parkin. Second, we examined the effect of 14-3-3η on the ubiquitylation of a model substrate for parkin. When V5-tagged synphilin-1, a known parkin substrate (Chung *et al*, 2001), was transfected with FL-parkin and HA-ubiquitin in the cells, V5-synphilin-1 was found in ubiquitylated form, as demonstrated by the poly-ubiquitin chain formation (detected by anti-HA antibody) in anti-V5 immunoprecipitant (Figure 3C, top panel). V5-synphilin-1 was not ubiquitylated when FL-parkin was not cotransfected, suggesting that this ubiquitylation is mediated by coexpressed FL-parkin. Indeed, FL-parkin was found to be associated with V5-synphilin-1, further supporting the above notion (Figure 3C, second panel from the top). Note that the polyubiquitylated bands observed as the smear profile were considered to include not only major synphilin-1 bands over 90-kDa size but also self-ubiquitylated bands of parkin over 52-kDa size.

In the next step, we tested the effects of 14-3-3η on the ubiquitylation and binding activities of parkin to

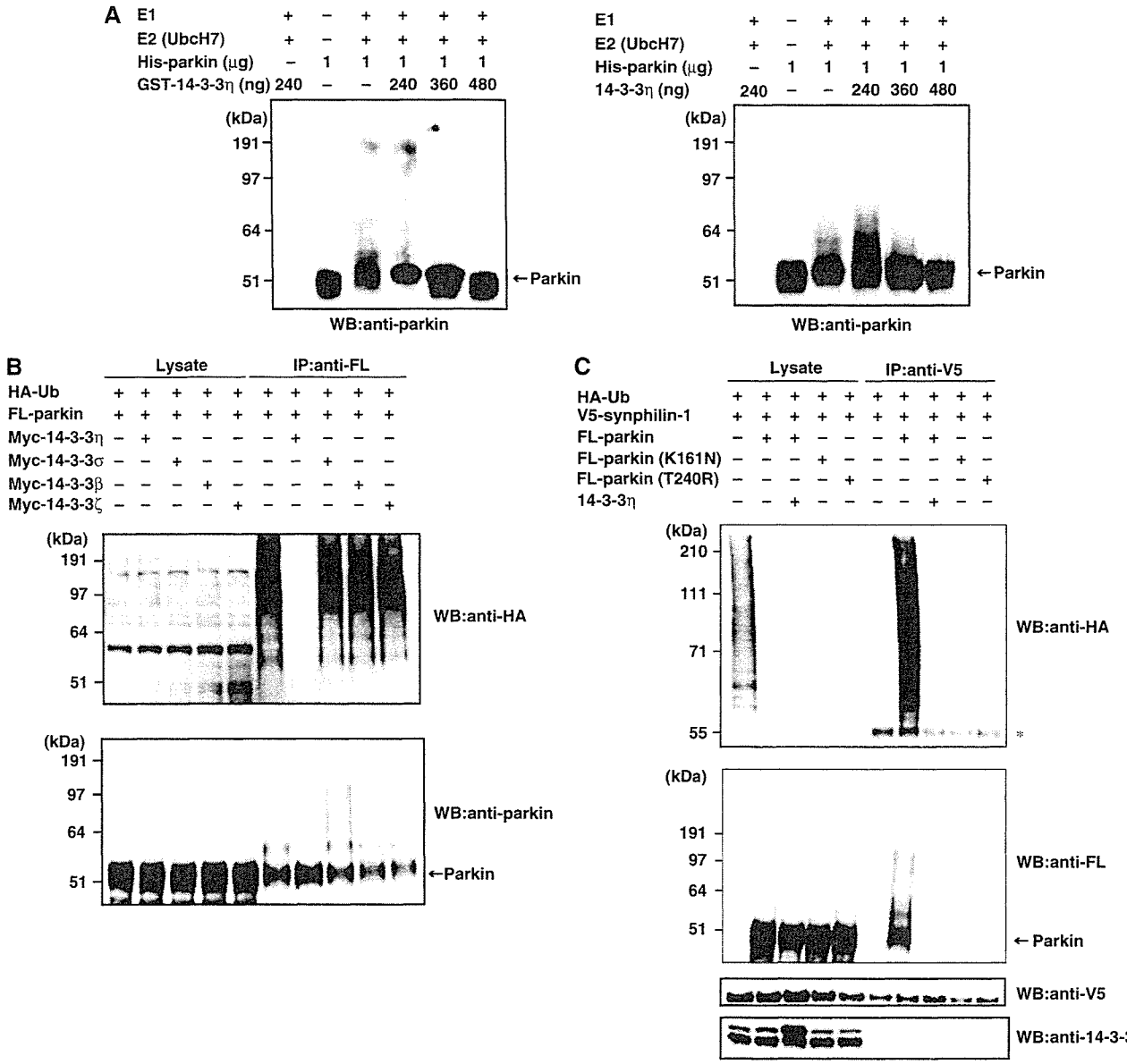

Figure 3 Effects of 14-3-3η on the E3 activity of parkin. (**A**) *In vitro* autoubiquitylation. The ubiquitylating assay was conducted as described in Materials and methods with or without various amounts of GST-14-3-3η (left panel) or 14-3-3η (right panel). After incubation, the reaction mixtures were subjected to SDS–PAGE, followed by Western blotting with anti-parkin. Arrow on the right indicates the position of His-parkin. (**B**) *In vivo* autoubiquitylation. HA-Ub (3 μg), FL-parkin (3 μg), and Myc-14-3-3η, σ, β, or ζ (6 μg) plasmids were transfected for 48 h into HEK293 cells as indicated. After immunoprecipitation with anti-FL, Western blotting was performed using antibodies against HA and parkin. Western blotting of all lysates was performed to test the expression levels (Lysate). (**C**) Ubiquitylation of synphilin-1 in HEK293 cells. HA-Ub (2 μg), FL-parkin (3 μg), FL-parkin(K161N) (3 μg), FL-parkin(T240R) (3 μg), Myc-14-3-3η (6 μg), and V5-synphilin-1 (4 μg) plasmids were transfected into HEK293 cells as in (B) at the indicated combinations. After immunoprecipitation with anti-V5 antibody, Western blotting was performed using antibodies against HA, FL, V5, and 14-3-3. Asterisk denotes an IgG heavy chain.

V5-synphilin-1. Cotransfection of 14-3-3η resulted in almost complete inhibition of the ubiquitylation of synphilin-1 by parkin and/or self-ubiquitylation of parkin (Figure 3C, top and second panels), as well as inhibition of the interaction between synphilin-1 and parkin (Figure 3C, second panel). 14-3-3η did not interact with synphilin-1 (Figure 3C, bottom panel). Taken together, these results suggest that 14-3-3η does not only inhibit the intrinsic ubiquitylation activity of parkin, but also its binding activity to the substrate and its ubiquitylation.

The ARJP disease-related parkin(K161N) and parkin(T240R) mutants, which cannot bind with 14-3-3η, could not bind and ubiquitylate synphilin-1 and/or self-ubiquitylation of parkin even in the absence of 14-3-3η (Figure 3C, top panel). Hence, the linker and RING-box domains of parkin are essential not only for the negative regulation by 14-3-3η, but also for the substrate recognition and ubiquitin-ligase activity. These results illustrate the importance of these regions of parkin on its positive and negative regulation.

Since parkin is known to associate with E2 (Shimura *et al*, 2000), we also examined the effect of 14-3-3η on the ability of parkin to recruit E2. For this purpose, we coexpressed HA-parkin with FL-UbcH7 or FL-Ubc7, both of which are known

to bind to parkin (Shimura *et al* 2000; Imai *et al*, 2001). Almost the same amounts of UbcH7 (Figure 4A) and Ubc7 (Figure 4B) were detected in the anti-parkin immunoprecipitants irrespective of cotransfection with Myc-14-3-3η. These findings indicate that 14-3-3η does not influence the recruitment of E2, that is, UbcH7 or Ubc7, to parkin.

α-Synuclein abrogates 14-3-3η-related parkin inactivation

Based on the above findings, we next examined the mechanism that regulates the 14-3-3η–parkin binding. As α-SN partly has a high homology to 14-3-3 isoforms (Ostrerova *et al*, 1999), we tested the effects of α-SN on the 14-3-3η-induced suppression of parkin. By cotransfection experiments in HEK293 cells, parkin again ubiquitylated synphilin-1, and 14-3-3η inhibited the parkin-mediated ubiquitylation (Figure 5A). Coexpression of α-SN resulted in the recovery of ubiquitylation of synphilin-1 and the association of synphilin-1 with parkin, suggesting that α-SN abrogates the 14-3-3η-induced suppression of parkin (Figure 5A, top panel). Importantly, the familial PD-related mutants of α-SN(A30P) (Kruger *et al*, 1998) and α-SN(A53T) (Polymeropoulos *et al*, 1997) could not abrogate the inhibitory role of 14-3-3η. Similar results were observed by detection of self-ubiquitylation activity of parkin (Figure 5A, second panel).

We then tested whether α-SN can release the binding of Myc-14-3-3η from parkin in cotransfection experiment. As shown in Figure 5B (top panel), FL-parkin was self-ubiquitylated in the absence of 14-3-3η. Coexpression of 14-3-3η inhibited the self-ubiquitylation of parkin, and this was accompanied by the binding of 14-3-3η to FL-parkin. Coexpression of α-SN abrogated the binding of 14-3-3η to parkin and resulted in the recovery of self-ubiquitylation of parkin. These effects were not seen by coexpression of α-SN(A30P) and α-SN(A53T) (Figure 5B, top panel). In addition, while the 14-3-3η–parkin interaction was considerably reduced by α-SN, it was not reduced by α-SN(A30P) or α-SN(A53T) (Figure 5B, bottom panel). Taken together, α-SN, but not α-SN(A30P) or α-SN(A53T), binds strongly to 14-3-3η and thereby releases parkin from the parkin–14-3-3η complex.

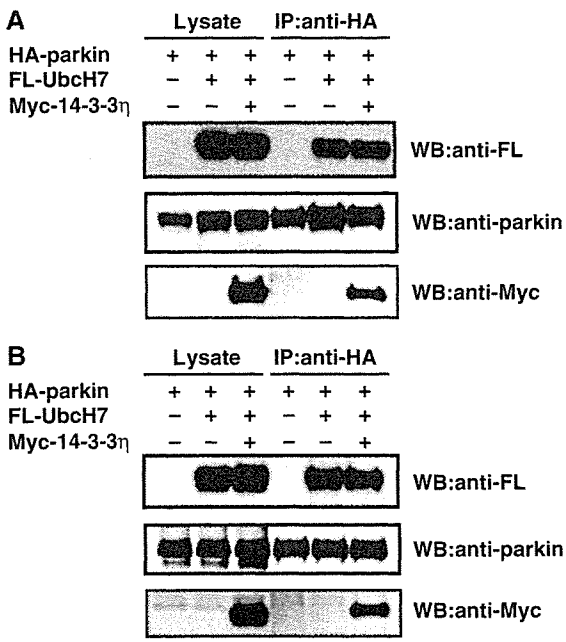

Figure 4 Effect of 14-3-3η on the recruitment of E2 (UbcH7 or Ubc7) to parkin. (**A**) HA-parkin (3 μg), FL-UbcH7 (3 μg), or Myc-14-3-3η (6 μg) plasmids were transfected for 48 h into HEK293 cells at the indicated combinations. After immunoprecipitation with anti-HA antibody, Western blotting was performed using antibodies against FL, Myc, and parkin. (**B**) The experiment was conducted as in (A), except that FL-Ubc7 was used instead of FL-UbcH7.

We also tested the interaction of Myc-14-3-3η with FL-α-SN, FL-α-SN(A30P), and FL-α-SN(A53T). Myc-14-3-3η interacted only with FL-α-SN, but not α-SN(A30P) nor α-SN(A53T) (Figure 5C, upper-top panel), suggesting that α-SN relieves parkin activity from binding to 14-3-3η. The 14-3-3η/α-SN interaction was not affected by parkin (Figure 5C, upper-top panel), and parkin was not associated with α-SN (Figure 5C, upper-second panel). Interestingly, FL-α-SN did not interact with Myc-14-3-3σ, β, and ζ in the same experiment (Figure 5C, lower panel). These results further strengthen the notion that α-SN specifically activates parkin through binding 14-3-3η.

We then investigated whether the interaction of 14-3-3η and parkin is direct or indirect by using purified recombinant His-parkin and GST-14-3-3η. GST or GST-14-3-3η was mixed with His-parkin, and pulled down by glutathione beads. His-parkin bound to GST-14-3-3η, but not GST (Figure 5D, left panel), indicating that parkin directly interacts with 14-3-3η. On the other hand, a similar *in vitro* binding assay showed that GST-14-3-3η did not interact with recombinant α-SN (Figure 5D, right panel), suggesting that certain modification(s) of α-SN may be required for the interaction of 14-3-3η.

Subsequently, we measured the binding affinities of parkin and α-SN for 14-3-3η by the surface plasmon resonance (SPR) method. As shown in Figure 5E, parkin bound 14-3-3η with a considerably strong affinity ($K_d = 4.2$ nM, upper), whereas the affinity of α-SN for 14-3-3η was much lower than that of parkin ($K_d = 1.1$ μM, lower). These results are consistent with those of the immunoprecipitation/Western analysis using recombinant proteins (Figure 5D).

Finally, we examined whether 14-3-3η bound to parkin can be released by α-SN. To test this, we first mixed the lysates coexpressing FL-parkin and Myc-14-3-3η of HEK293 cells with those expressing α-SN. Then the mixtures were incubated under three different conditions, as indicated in the upper panel of Figure 5F. Next, the lysates were immunoprecipitated with anti-FL antibody, and followed by Western blotting with anti-Myc and anti-parkin antibodies. As shown in Figure 5F (upper panel), the amount of 14-3-3η bound to parkin was significantly lower in all incubation conditions, when the cell lysates that simultaneously expressed both parkin and 14-3-3η were incubated with α-SN-expressing lysates. Incubation for 1 h at 37°C reduced the amount of 14-3-3η bound to parkin in proportion to the added amount of α-SN-expressing cell lysate (Figure 5F, lower panel). Intriguingly, the α-SN(A30P) and α-SN(A53T) mutants had no effect on the release of 14-3-3η, unlike wild-type (WT) α-SN (Figure 5F, lower panel). These observations strongly indicate that α-SN, but not α-SN(A30P) or α-SN(A53T), can capture and release 14-3-3η from the parkin–14-3-3η complex, which supports our notion that the negative regulation of parkin activity by 14-3-3η is relieved by α-SN (Figure 5A and B).

Parkin, 14-3-3η, and α-SN levels in the substantia nigra of PD

Finally, we analyzed the levels of parkin, 14-3-3η, and α-SN in the substantia nigra of the midbrain from patients with sporadic PD. Western blotting revealed no significant differences in parkin, 14-3-3η, and actin in the substantia nigra between control (patients without PD) and PD patients, whereas α-SN was significantly increased in the substantia nigra of PD patients (Figure 6A, upper panel). As parkin did not interact physically with α-SN in our immunoprecipitation analysis (Figure 5C; data not shown), we then examined the interactions of 14-3-3η with parkin or α-SN by measuring

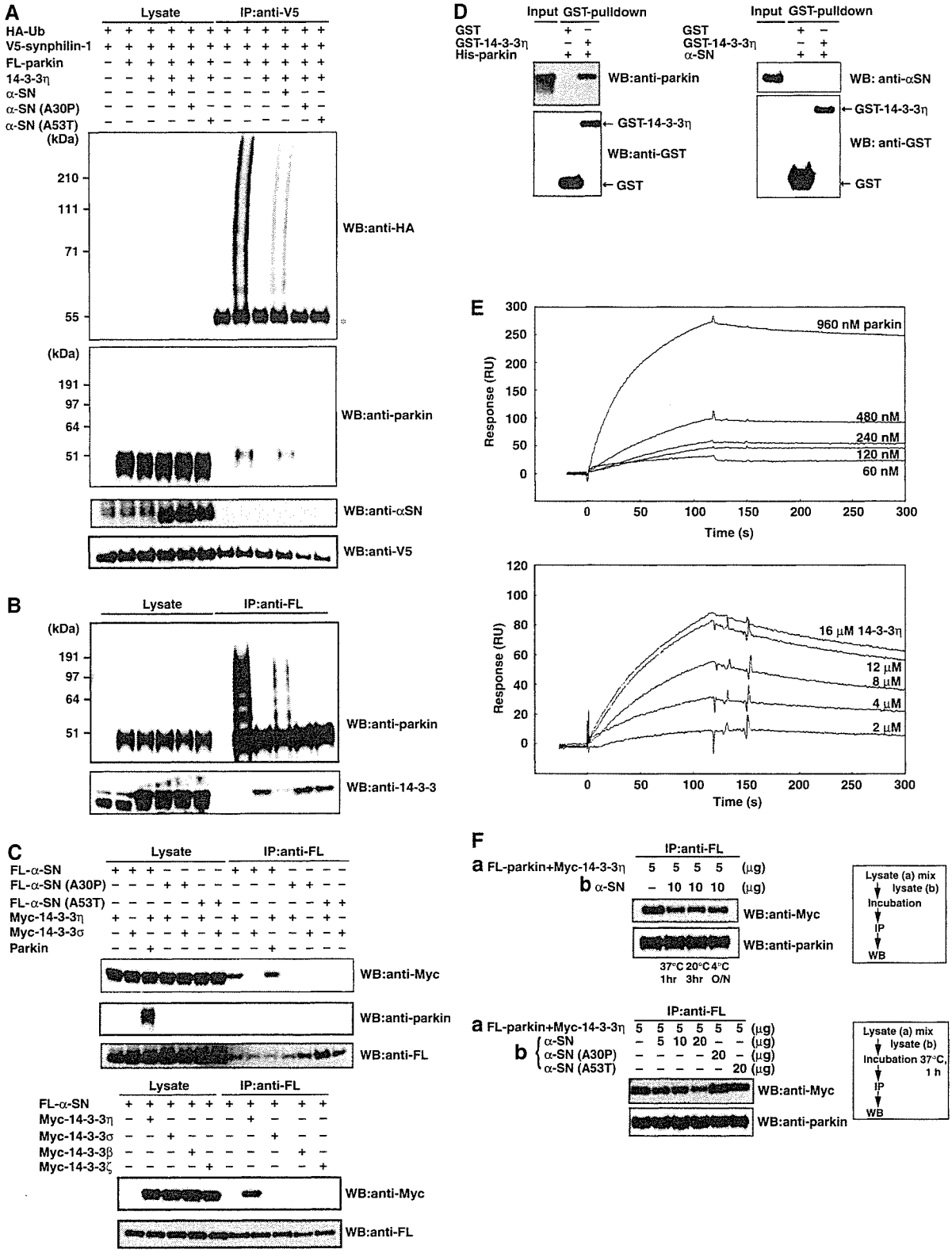

these proteins in the anti-14-3-3η immunoprecipitant. Whereas the levels of parkin associated with 14-3-3η from PD appeared to be decreased relative to the control, the levels of α-SN that interacted with 14-3-3η were clearly increased in patients with PD (Figure 6A, lower panel). Thus, it is suggested that the elevated levels of α-SN are associated with its interaction with 14-3-3η and the activity of parkin may be aberrantly regulated in the substantia nigra of sporadic PD.

Discussion

The major finding of the present study was the identification of 14-3-3η as a novel regulator of parkin. First, parkin was in a complex with 14-3-3η, but not β, γ, ε, or τ isoforms, in the mouse brain (Figure 1). 14-3-3η could bind primarily to the linker region of parkin, but not with the ARJP-causing missense mutant parkin (K161N), which has a mutation in the

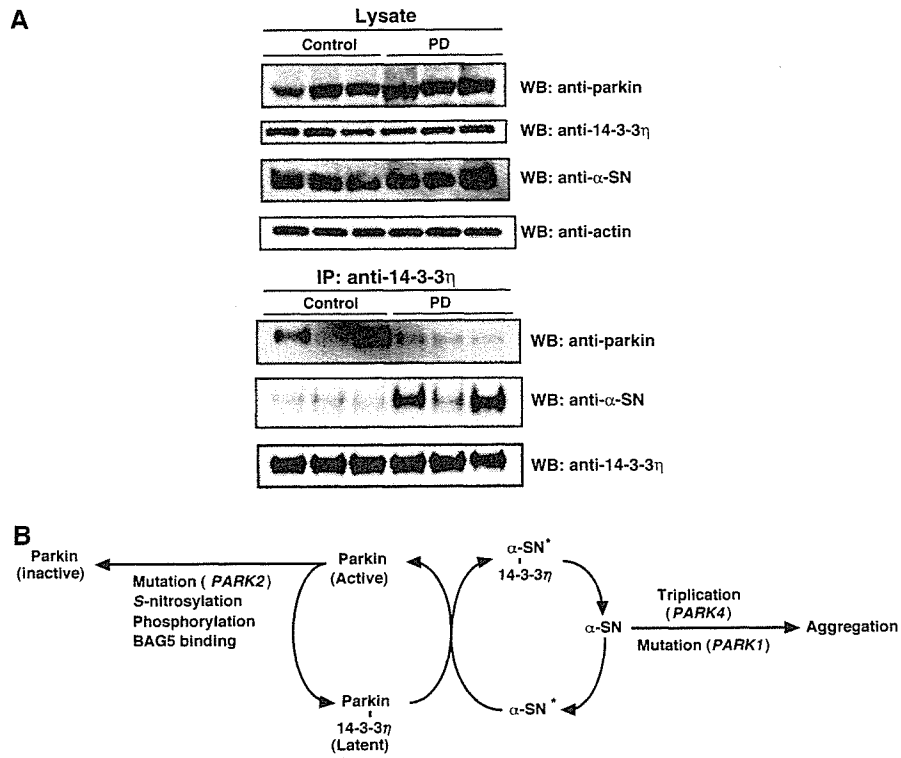

Figure 6 (**A**) Levels of parkin, 14-3-3η, and α-SN in the substantia nigra of PD. Brain of a representative patient with PD (upper panel). Samples (30 μg) of the crude extract of the brains (substantia nigra) of control (patients without PD) and PD patients were subjected to SDS–PAGE, following Western blotting against antibodies against parkin, 14-3-3η, α-SN, and actin. Physical interaction between 14-3-3η and parkin or α-SN (lower panel). After the same samples used in the upper panel were immunoprecipitated with anti-14-3-3η, Western blotting was carried out using antibodies against parkin, α-SN, and 14-3-3η. (**B**) A schematic diagram showing the pathways involved in the regulation of parkin activity by 14-3-3η and α-SN. α-SN, α-synuclein; α-SN*, modified form of α-SN. Note that whether parkin is phosphorylated to bind to 14-3-3η remains unknown at present. See text for details.

Figure 5 Effects of α-SN on 14-3-3η-induced suppression of parkin E3 activity and interaction between 14-3-3η and α-SN in HEK293 cells. (**A**) Ubiquitylation of synphilin-1. Transfection was conducted at various combinations, as in Figure 3C, except for cotransfection of 4 μg of α-SN, α-SN(A30P), and α-SN(A53T). After immunoprecipitation with anti-V5 antibody, Western blotting was carried out with antibodies against HA, parkin and α-SN, and V5. Asterisk denotes an IgG heavy chain. (**B**) Autoubiquitylation of parkin. Transfection was performed as in (A). After immunoprecipitation with anti-FL antibody, Western blotting was carried out with antibodies against parkin and 14-3-3. (**C**) Interaction of 14-3-3η and α-SN with or without parkin. Various expression vectors at the indicated combinations were transfected. Immunoprecipitation was conducted by anti-FL antibody and the resulting immunoprecipitates were used for Western blotting with antibodies against Myc, parkin, and FL. (**D**) Physical interaction between 14-3-3η and parkin (left panel) or α-SN (right panel) in recombinant proteins. After recombinant His-tagged parkin produced from baculovirus-infected HiFive insect cells (3 μg) or GST-α-SN expressed in *E. coli* whose GST moiety was removed by PreScission Protease digestion prior to use (3 μg) was incubated for 1 h at 32°C with 3 μg of GST or GST-tagged 14-3-3η expressed in *E. coli*, glutathione-Sepharose was added and the incubation vessels were slowly rotated for 3 h at 4°C. The washed Sepharose resin was eluted with 50 μl of 50 mM Tris–HCl (pH 8.0) buffer containing 10 mM reduced glutathione, and aliquots (15 μl) were analyzed by Western blotting with antibodies against parkin (left-top panel), α-SN (right-top panel), and GST (bottom panel). Input: 500 ng of parkin or α-SN. (**E**) SPR analyses of parkin and α-SN binding to 14-3-3η. Upper: subtracted sensorgrams of interaction between a subset of parkin concentrations and immobilized 14-3-3η. Lower: subtracted sensorgrams of interaction between a subset of 14-3-3η concentrations and immobilized α-SN. (**F**) Sequestration of 14-3-3η by α-SN from the parkin–14-3-3η complex. Various expression vectors were transfected as indicated. Upper panel: 5 μg of the lysate-(a) from cells co-expressing FL-parkin and Myc-14-3-3η were mixed with 10 μg of cellular lysate-(b) expressing α-SN. The mixtures were incubated under various conditions; that is, 37°C for 1 h, 20°C for 3 h, or overnight at 4°C (O/N), then immunoprecipitation by anti-FL antibody was conducted, followed by Western blotting with antibodies against Myc (14-3-3η) and parkin. Lower panel: the experiments were conducted as for the top panel, except that incubation was carried out at 37°C for 1 h using α-SN-, α-SN(A30P)-, or α-SN (A53T)-expressing lysates as indicated. The experimental protocol is shown in the flow charts on the right.

linker region (Figure 2). Second, the binding of 14-3-3η to parkin was associated with suppression of the ubiquitin-ligase activity, suggesting that certain parkin bound to 14-3-3η is present at a latent status in the brain (Figure 3). Third, overexpression of α-SN abrogated the 14-3-3η-induced suppression of parkin activity, indicating that α-SN relieves the negative regulation of parkin by 14-3-3η (Figure 5A and B). Intriguingly, PD-causing A30P and A53T mutations of α-SN could not bind 14-3-3η and failed to activate parkin. These results indicate that 14-3-3η is a regulator that functionally links parkin and α-SN, as illustrated in Figure 6B.

It is of particular note that we report unusual isoform specificity for 14-3-3η to interact with parkin among all 14-3-3 species examined. However, the possibility that the other species are also involved in the interaction by forming a heterodimer with 14-3-3η cannot be excluded *in vivo*, because 14-3-3 bands immunoprecipitated by anti-parkin antibody from the brain extracts showed doublet with one weak signal for Western blotting (Figure 1A). Nevertheless, herein we address that recombinant parkin could directly bind to 14-3-3η (Figure 5D, left panel), with considerably high affinity (K_d = approximately 4 nM) (Figure 5E) and that the 14-3-3η homodimer is a negative factor for autoubiquitylating activity of parkin *in vitro* (Figure 3A).

It is known that the 14-3-3 family proteins interact with the majority, but not all, proteins after their phosphorylation (Aitken *et al*, 2002; Bridges and Moorhead, 2004; Mackintosh, 2004). Indeed, parkin contains the RKDSPP sequence in the linker region that resembles the typical binding motifs with a potential phosphorylation residue for 14-3-3 proteins (Yaffe *et al*, 1997; Mackintosh, 2004). It is also known that parkin has several possible phosphorylation sites, and recent studies showed that parkin is phosphorylated *in vitro* (Yamamoto *et al*, 2004), although there is no direct evidence demonstrating phosphorylation of parkin *in vivo* to date. However, it remains elusive whether or not phosphorylation of parkin is responsible for its specific binding to 14-3-3η, because known potential phosphorylation motifs are capable of associating with many 14-3-3 species in general. The specificities of 14-3-3: client–protein interactions do not result from different specificities for the phosphopeptide-binding motifs, but probably arises from contacts made on the variable surface of 14-3-3 outside the binding cleft, as discussed previously by Yaffe *et al* (1997). In this regard, some reports showed functional specificities of 14-3-3 isoforms (Aitken, 2002; Aitken *et al*, 2002; Roberts and de Bruxelles, 2002), and indeed several enzymes retain several nonphosphorylated binding motifs for 14-3-3s (Hallberg, 2002; Sribar *et al*, 2003), though parkin lacks such 14-3-3-interacting sequences. Thus, parkin, in particular its linker region, may have a new binding motif(s) for 14-3-3η, but the interacting motif(s) remains to be identified. If 14-3-3η binds to parkin through two sites as a dimmer, it is plausible that the phosphorylation of parkin is involved in their interactions at least in part.

With regard to the mechanistic action of 14-3-3η, it may suppress parkin activity by preventing access of the substrate, because the binding of synphilin-1 (used here as a model substrate to parkin) was inhibited by 14-3-3η (Figure 3C). Accumulating evidence suggests that parkin can bind various targets by the UBL domain or the RING box, in particular the RING 1 domain (Dawson and Dawson, 2003). Accordingly, 14-3-3η may have function(s) other than suppressing the access of the substrate to parkin. Indeed, 14-3-3η strongly inhibits substrate-independent self-ubiquitylation of parkin, indicating blockage of the intrinsic E3 activity. It was also anticipated that 14-3-3η hinders the recruitment of E2 to parkin. However, this was not the case, because 14-3-3η had no effect on the binding of UbcH7 and Ubc7 to parkin (Figure 4). Thus, while the mechanism of 14-3-3η-induced suppression of parkin activity remains to be identified, it is possible that it involves preventing the positioning of the ubiquitin-charged E2 toward the target Lys residue by steric hindrance due to the association of 14-3-3η to parkin.

It is worth noting that parkin does not interact with α-SN directly, because we could not demonstrate the physical binding of parkin to α-SN *in vivo* and *in vitro* (data not shown; see also Dawson and Dawson, 2003). Nevertheless, we found that the negative regulation of parkin by 14-3-3η was relieved by α-SN, which could bind tightly to 14-3-3η *in vivo* (Figure 5A–C). In this regard, it is of note that the amounts of 14-3-3η bound to parkin were decreased when the lysates of cells coexpressing parkin and 14-3-3η were incubated with those expressing WT α-SN, but not PD-related α-SN(A30P) or α-SN(A53T) mutants *in vitro* (Figure 5F). These results clearly indicate that 14-3-3η bound to parkin is sequestered by α-SN, but not competition by α-SN toward the binding of 14-3-3η to parkin. Unlike the association between parkin and 14-3-3η, there is little or no interaction between α-SN and 14-3-3η *in vitro*, as recombinant α-SN did not bind to 14-3-3η (Figure 5D, right panel, and E). Thus, it is plausible that certain modification(s) of α-SN is required for its association to 14-3-3η in mammalian cells (see our model in Figure 6B). Judging from the characteristic properties of 14-3-3 family proteins capable of binding many phosphorylated proteins (Yaffe *et al*, 1997), certain phosphorylation(s) of α-SN seems quite possible for the interaction with 14-3-3η. Indeed, there are several reports regarding phosphorylation of α-SN (Fujiwara *et al*, 2002; Hirai *et al*, 2004). Although previous studies clearly demonstrated that α-SN deposited in synucleinopathy brains is extensively phosphorylated at Ser-129 (Fujiwara *et al*, 2002; Hirai *et al*, 2004), this is probably not the case in our study, because the chemically synthesized peptide phosphorylated at Ser-129 of α-SN did not bind to the 14-3-3η (our unpublished results). However, the possibility that α-SN is phosphorylated at other site(s) cannot be exclusively ruled out. Alternatively, one cannot exclude a possible, though yet unknown, modification(s) of α-SN other than phosphorylation as a mechanism responsible for the increased affinity toward 14-3-3η. In this regard, α-SN is structurally related to 14-3-3 family proteins (Ostrerova *et al*, 1999), but it is unknown whether the homologous region is involved in the physical interaction with α-SN. Further studies are required to clarify the mode of α-SN modification.

In the present study, we found reciprocal regulation of parkin activity by α-SN and 14-3-3η, whose tripartite control could enhance our understanding of the pathogenesis of PD. As illustrated in Figure 6B, to date there are several reports on the post-translational modification of parkin. Recent findings indicate that the ubiquitin E3 ligase activity of parkin is modified by nitric oxide (NO). Namely, parkin is *S*-nitrosylated in PD patients and an *in vivo* mouse model of PD, and *S*-nitrosylation shows inhibition of the E3 activity of

parkin (Chung *et al*, 2004; Kahle and Haass, 2004; Yao *et al*, 2004), which could contribute to the degenerative process in PD by impairing the ubiquitylation of parkin substrates. Moreover, Kalia *et al* (2004) showed that the bcl-2-associated athanogene 5 (BAG5) enhanced the death of dopaminergic neurons in an *in vivo* model of PD by inhibiting the E3 ligase activity of parkin. In addition, recent studies reported that phosphorylation of parkin causes a small but significant reduction of parkin auto-ubiquitylating activity (Yamamoto *et al*, 2004). More recently, it was reported that Nrdp1/FLRF RING-finger E3 ligase binds and ubiquitylates parkin, resulting in reduction of parkin activity, implying its involvement in the pathogenesis of PD (Zhong *et al*, 2005). Considered together, these results indicate that the apparent loss of parkin E3 ubiquitin ligase activity associated with the pathogenesis of PD (see the model displayed in Figure 6B) is in agreement with the ARJP-linked mutations that lead to loss of function of parkin, and that the functional loss of parkin activity is linked to the death of dopaminergic neurons. In addition, we reported herein the imbalance of tripartite interactions among parkin, 14-3-3η, and α-SN levels in the substantia nigra of sporadic PD, but it is still not clear how these alterations influence parkin activity in neural cells. Thus, parkin is an E3 ubiquitin ligase involved in the ubiquitylation of proteins, irrespective of its involvement of K48- or K63-linked ubiquitylation (Doss-Pepe *et al*, 2005; Lim *et al*, 2005), that are important in the survival of dopaminergic neurons in PD.

In the present study, we found that parkin E3 activity is regulated positively and negatively by α-SN and 14-3-3η, respectively, suggesting that derangements of this regulation may be responsible for ARJP. For instance, the activated parkin free from 14-3-3η may be labile, and thus sensitive to other stresses, such as *S*-nitrosylation, and inactivated secondarily in PD. This situation resembles the effect of *S*-nitrosylation, in which nitrosative stress leads to *S*-nitrosylation of WT parkin, which leads initially to a marked increase followed by a decrease in the E3 ligase–ubiquitin–proteasome degradative pathway (Yao *et al*, 2004). The initial increase in the activity of parkin's E3 ubiquitin ligase leads to autoubiquitylation of parkin and subsequent inhibition of its activity, which would impair ubiquitylation and clearance of parkin substrates. In turn, 14-3-3η may protect against impairment of parkin induced by various environmental stresses, including *S*-nitrosylation. It is also noteworthy that, although 14-3-3η acts as a negative regulator of parkin, it may play a positive role in maintaining a large pool of parkin by preventing its self-ubiquitylation in the brain. Finally, we assume that gradual reduction of parkin activity may be associated with the development of ARJP as well as sporadic PD.

Current evidence suggests that α-SN increases in response to various stresses (Sherer *et al*, 2002; Gomez-Santos *et al*, 2003). This finding is compatible with the results of recent studies that dopamine-dependent neurotoxicity (Tabrizi *et al*, 2000; Zhou *et al*, 2000; Junn and Mouradian, 2002) is mediated by the formation of protein complexes that contain α-SN and 14-3-3, which are selectively increased in the substantia nigra in PD (Xu *et al*, 2002). Further studies are needed to determine the levels of parkin, 14-3-3η, α-SN, and parkin and α-SN-14-3-3η complexes in the substantia nigra of the midbrain of patients with sporadic PD.

Here we suggest that α-SN and parkin function through the same pathway. Indeed, both proteins, if not all, are associated with presynaptic vesicles (Dawson and Dawson, 2003). So far, however, the physiological role of α-SN is largely unknown, though various roles including its involvement in synaptic plasticity have been suggested (Liu *et al*, 2004). We here provided the first evidence that α-SN acts as a positive regulator of parkin E3 activity. It is worth noting that disease-causing mutations of α-SN(A30P) and α-SN(A53T) could not activate the latent parkin–14-3-3η complex, and thus, these mutations may accelerate the development of PD by failing to activate parkin. Our results identified a functional link between these two familial PD-gene products, thus highlighting the existence of a novel regulatory mechanism that could help us further understand the pathogenesis of ARJP as well as sporadic PD. However, it must be stressed here that α-SN is the causative gene product of familial PD. It is noteworthy that α-SN is an aggregation-prone protein due to its natively unfolded protein nature. It is of note that the locus of *PARK4* is triplication of the α-*SN* gene (*PARK1*) (Singleton *et al*, 2003), indicating that overexpression of α-SN itself is toxic and induces dopaminergic neuronal death. Indeed, α-SN tends to self-aggregate, and this tendency, which is augmented in the α-SN(A30P) and α-SN(A53T) mutants (Conway *et al*, 2000) (see our model in Figure 6B), causes autosomal dominant PD (Narhi *et al*, 1999). Both WT and mutant α-SN form amyloid fibrils akin to those seen in LBs, as well as nonfibrillary oligomers termed protofibrils (Dawson and Dawson, 2003; Bossy-Wetzel *et al*, 2004). However, whether aggregation and fibrillary formation of α-SN- and PD-linked mutants play a role in neuronal dysfunction and death of neurons in PD are a matter of fierce debate. At this point of view, we emphasize that the feature of α-SN as an aggregation-prone protein is probably not linked directly to its role as a potent activator of parkin E3 in the pathogenesis of PD. Even if these two unique properties of α-SN account for the development of PD independently or synergistically, however, it is clear that their mechanistic actions differ as illustrated in Figure 6B.

Materials and methods

Immunological analysis

For immunoprecipitation analysis of endogenous proteins in the brains of adult mouse and human, these brains were homogenized in three volumes of ice-cold lysis buffer (20 mM HEPES (pH 7.9) buffer containing 0.2% NP-40, 1 mM dithiothreitol (DTT) and protease inhibitor cocktail (Sigma, Chemical Co., St Louis, MO)). The tissue homogenate was centrifuged at 20 000*g* at 4°C for 20 min. The supernatant (2 mg protein) was used for immunoprecipitation with one of the following antibodies: anti-polyclonal parkin (Cell Signaling Technology, Beverly, MA) and anti-14-3-3η antibodies (Immuno-Biological Lab. Co., Gunma) or control IgG (700 ng). The resulting immunoprecipitates were resolved in 30 μl of the sodium dodecyl sulfate–polyacrylamide gel electrophoresis (SDS–PAGE) sample buffer, and one-third of the samples (10 μl) were subjected to SDS–PAGE, followed by Western blotting with anti-14-3-3 (Santa Cruz Biotechnology, Santa Cruz, CA), anti-14-3-3β, 14-3-3γ, 14-3-3ε, 14-3-3η, and 14-3-3τ (Immuno-Biological Lab. Co., Ltd, Japan) and anti-monoclonal parkin (1A1) antibodies (Shimura *et al*, 1999). In all, 10 μg of the supernatant (lysate) was used as input (1.5%).

For immunoprecipitation analysis of the cell culture system, HEK293 cells were transfected with the respective plasmids. After 48 h, the cells were washed with ice-cold PBS (in mM, 10 Na_2PO_4, 2 KH_2PO_4, 137 NaCl, and 2.7 KCl), pH 7.4, and harvested in the lysis buffer (600 μl). The lysate was then rotated at 4°C for 1 h, followed by centrifugation at 20 000*g* for 10 min. The supernatant (200 μl) was then combined with 50 μl protein G-Sepharose (Amersham Life

Science, Buckinghamshire, UK), pre-incubated with anti-Myc (Santa Cruz Biotechnology, Santa Cruz), V5 (Invitrogen), and HA (Santa Cruz Biotechnology) antibodies or anti-FL antibody beads (Sigma) for 3 h. The protein G-Sepharose or FL-beads were precipitated and the pellets were extensively washed using the lysis buffer containing 500 mM NaCl. The precipitates were used for Western blot analysis using anti-parkin, Myc, FL, HA, V5, 14-3-3, and α-SN (BD Transduction Lab.) antibodies, as mentioned above. A volume of 5 μl of the supernatant was used as input (7.5%).

In vitro autoubiquitylation assay

Recombinant GST-14-3-3η was produced in *Escherichia coli*. Untagged 14-3-3η was produced from GST-14-3-3η by digestion with PreScission Protease (Amersham Bioscience). Recombinant His-parkin and E1 were produced from baculovirus-infected HiFive insect cells. Reactions were performed for 3 h at 37°C in 50 μl of assay mixture containing 40 mM Tris–HCl buffer (pH 7.5), 5 mM $MgCl_2$, 2 mM ATP, 2 mM DTT, 15 μg ubiquitin (Sigma), 200 ng of E1, and 600 ng of E2 (UbcH7) (Affiniti-Research, Exeter, Devon, UK) in the presence or absence of GST-14-3-3η or 14-3-3η. After incubation, the reaction was terminated by the addition of the sample buffer for SDS–PAGE (17 μl), and aliquots (15 μl) were subjected to SDS–PAGE followed by Western blotting with anti-parkin antibody.

In vivo ubiquitylation assay

HEK293 cells were transfected for 48 h with pcDNA3.1 expression plasmids, in which FL-tagged parkin or FL-parkin mutants, α-SN or α-SN mutants, 14-3-3η, V5-synphilin-1, and HA-ubiquitin cDNAs were ligated. MG132 (50 μM) was added for 20 min, prior to harvesting of the cells. Then, the cells were washed with cold PBS and lysed by 50 mM Tris–HCl buffer (pH 8.0), containing 150 mM NaCl, 1% Nonidet-P40, 1% deoxycolate, 0.1% SDS, 5 mM ethylenediaminetetraacetic acid, and protease inhibitor cocktail. Preparation of the cell lysate, immunoprecipitation, and Western blot analyses were essentially the same for the immunological analysis as described above. In all experiments, the cell lysates (10 μg, 7.5% input) were used for Western blotting as controls to check the expression levels.

For the method sections of 'Cell culture and transfection', 'Plasmids', and 'Surface plasmon resonance (SPR) analysis', see Supplementary data.

Supplementary data

Supplementary data are available at *The EMBO Journal* Online.

Acknowledgements

We thank Y Goto for providing the 14-3-3σ, β, and ζ expression plasmids, and T Ichimura for the valuable discussion. This work was supported in part by Grants-in-Aid from the Ministry of Education, Culture, Sports, Science and Technology of Japan.

References

Aitken A (2002) Functional specificity in 14-3-3 isoform interactions through dimer formation and phosphorylation. Chromosome location of mammalian isoforms and variants. *Plant Mol Biol* **50:** 993–1010

Aitken A, Baxter H, Dubois T, Clokie S, Mackie S, Mitchell K, Peden A, Zemlickova E (2002) Specificity of 14-3-3 isoform dimer interactions and phosphorylation. *Biochem Soc Trans* **30:** 351–360

Baxter HC, Liu WG, Forster JL, Aitken A, Fraser JR (2002) Immunolocalisation of 14-3-3 isoforms in normal and scrapie-infected murine brain. *Neuroscience* **109:** 5–14

Berg D, Holzmann C, Riess O (2003) 14-3-3 proteins in the nervous system. *Nat Rev Neurosci* **4:** 752–762

Bossy-Wetzel E, Schwarzenbacher R, Lipton SA (2004) Molecular pathways to neurodegeneration. *Nat Med* **10** (Suppl S2): S2–S9

Bridges D, Moorhead GB (2004) 14-3-3 proteins: a number of functions for a numbered protein. *Sci STKE* **2004:** re10

Chung KK, Thomas B, Li X, Pletnikova O, Troncoso JC, Marsh L, Dawson VL, Dawson TM (2004) *S*-nitrosylation of parkin regulates ubiquitination and compromises parkin's protective function. *Science* **304:** 1328–1331

Chung KK, Zhang Y, Lim KL, Tanaka Y, Huang H, Gao J, Ross CA, Dawson VL, Dawson TM (2001) Parkin ubiquitinates the α-synuclein-interacting protein, synphilin-1: implications for Lewy-body formation in Parkinson disease. *Nat Med* **7:** 1144–1150

Conway KA, Lee SJ, Rochet JC, Ding TT, Williamson RE, Lansbury Jr PT (2000) Acceleration of oligomerization, not fibrillization, is a shared property of both α-synuclein mutations linked to early-onset Parkinson's disease: implications for pathogenesis and therapy. *Proc Natl Acad Sci USA* **97:** 571–576

Dawson TM, Dawson VL (2003) Molecular pathways of neurodegeneration in Parkinson's disease. *Science* **302:** 819–822

Doss-Pepe EW, Chen L, Madura K (2005) α-Synuclein and parkin contribute to the assembly of ubiquitin lysine 63-linked multiubiquitin chains. *J Biol Chem* **280:** 16619–16624

Forno LS (1996) Neuropathology of Parkinson's disease. *J Neuropathol Exp Neurol* **55:** 259–272

Fujiwara H, Hasegawa M, Dohmae N, Kawashima A, Masliah E, Goldberg MS, Shen J, Takio K, Iwatsubo T (2002) α-Synuclein is phosphorylated in synucleinopathy lesions. *Nat Cell Biol* **4:** 160–164

Gomez-Santos C, Ferrer I, Santidrian AF, Barrachina M, Gil J, Ambrosio S (2003) Dopamine induces autophagic cell death and α-synuclein increase in human neuroblastoma SH-SY5Y cells. *J Neurosci Res* **73:** 341–350

Hallberg B (2002) Exoenzyme S binds its cofactor 14-3-3 through a non-phosphorylated motif. *Biochem Soc Trans* **30:** 401–405

Hirai Y, Fujita SC, Iwatsubo T, Hasegawa M (2004) Phosphorylated α-synuclein in normal mouse brain. *FEBS Lett* **572:** 227–232

Imai Y, Soda M, Inoue H, Hattori N, Mizuno Y, Takahashi R (2001) An unfolded putative transmembrane polypeptide, which can lead to endoplasmic reticulum stress, is a substrate of Parkin. *Cell* **105:** 891–902

Junn E, Mouradian MM (2002) Human α-synuclein over-expression increases intracellular reactive oxygen species levels and susceptibility to dopamine. *Neurosci Lett* **320:** 146–150

Kahle PJ, Haass C (2004) How does parkin ligate ubiquitin to Parkinson's disease? *EMBO Rep* **5:** 681–685

Kalia SK, Lee S, Smith PD, Liu L, Crocker SJ, Thorarinsdottir TE, Glover JR, Fon EA, Park DS, Lozano AM (2004) BAG5 inhibits parkin and enhances dopaminergic neuron degeneration. *Neuron* **44:** 931–945

Kawakami T, Chiba T, Suzuki T, Iwai K, Yamanaka K, Minato N, Suzuki H, Shimbara N, Hidaka Y, Osaka F, Omata M, Tanaka K (2001) NEDD8 recruits E2-ubiquitin to SCF E3 ligase. *EMBO J* **20:** 4003–4012

Kawamoto Y, Akiguchi I, Nakamura S, Honjyo Y, Shibasaki H, Budka H (2002) 14-3-3 proteins in Lewy bodies in Parkinson disease and diffuse Lewy body disease brains. *J Neuropathol Exp Neurol* **61:** 245–253

Kruger R, Kuhn W, Muller T, Woitalla D, Graeber M, Kosel S, Przuntek H, Epplen JT, Schols L, Riess O (1998) A30P mutation in the gene encoding α-synuclein in Parkinson's disease. *Nat Genet* **18:** 106–108

Lim KL, Chew KC, Tan JM, Wang C, Chung KK, Zhang Y, Tanaka Y, Smith W, Engelender S, Ross CA, Dawson VL, Dawson TM (2005) Parkin mediates nonclassical, proteasomal-independent ubiquitination of synphilin-1: implications for Lewy body formation. *J Neurosci* **25:** 2002–2009

Liu S, Ninan I, Antonova I, Battaglia F, Trinchese F, Narasanna A, Kolodilov N, Dauer W, Hawkins RD, Arancio O (2004) Synuclein produces a long-lasting increase in neurotransmitter release. *EMBO J* **23:** 4506–4516

Mackintosh C (2004) Dynamic interactions between 14-3-3 proteins and phosphoproteins regulate diverse cellular processes. *Biochem J* **381:** 329–342

Martin H, Rostas J, Patel Y, Aitken A (1994) Subcellular localisation of 14-3-3 isoforms in rat brain using specific antibodies. *J Neurochem* **63:** 2259–2265

McNaught KS, Olanow CW (2003) Proteolytic stress: a unifying concept for the etiopathogenesis of Parkinson's disease. *Ann Neurol* **53** (Suppl 3): S73–S84

Narhi L, Wood SJ, Steavenson S, Jiang Y, Wu GM, Anafi D, Kaufman SA, Martin F, Sitney K, Denis P, Louis JC, Wypych J, Biere AL, Citron M. (1999) Both familial Parkinson's disease mutations accelerate α-synuclein aggregation. *J Biol Chem* **274:** 9843–9846

Ostrerova N, Petrucelli L, Farrer M, Mehta N, Choi P, Hardy J, Wolozin B (1999) α-Synuclein shares physical and functional homology with 14-3-3 proteins. *J Neurosci* **19:** 5782–5791

Polymeropoulos MH, Lavedan C, Leroy E, Ide SE, Dehejia A, Dutra A, Pike B, Root H, Rubenstein J, Boyer R, Stenroos ES, Chandrasekharappa S, Athanassiadou A, Papapetropoulos T, Johnson WG, Lazzarini AM, Duvoisin RC, Di Iorio G, Golbe LI, Nussbaum RL (1997) Mutation in the α-synuclein gene identified in families with Parkinson's disease. *Science* **276:** 2045–2047

Roberts MR, de Bruxelles GL (2002) Plant 14-3-3 protein families: evidence for isoform-specific functions? *Biochem Soc Trans* **30:** 373–378

Sherer TB, Betarbet R, Stout AK, Lund S, Baptista M, Panov AV, Cookson MR, Greenamyre JT (2002) An *in vitro* model of Parkinson's disease: linking mitochondrial impairment to altered α-synuclein metabolism and oxidative damage. *J Neurosci* **22:** 7006–7015

Shimura H, Hattori N, Kubo S, Mizuno Y, Asakawa S, Minoshima S, Shimizu N, Iwai K, Chiba T, Tanaka K, Suzuki T (2000) Familial Parkinson disease gene product, parkin, is a ubiquitin-protein ligase. *Nat Genet* **25:** 302–305

Shimura H, Hattori N, Kubo S, Yoshikawa M, Kitada T, Matsumine H, Asakawa S, Minoshima S, Yamamura Y, Shimizu N, Mizuno Y (1999) Immunohistochemical and subcellular localization of Parkin protein: absence of protein in autosomal recessive juvenile parkinsonism patients. *Ann Neurol* **45:** 668–672

Singleton AB, Farrer M, Johnson J, Singleton A, Hague S, Kachergus J, Hulihan M, Peuralinna T, Dutra A, Nussbaum R, Lincoln S, Crawley A, Hanson M, Maraganore D, Adler C, Cookson MR, Muenter M, Baptista M, Miller D, Blancato J, Hardy J, Gwinn-Hardy K (2003) α-Synuclein locus triplication causes Parkinson's disease. *Science* **302:** 841

Sribar J, Sherman NE, Prijatelj P, Faure G, Gubensek F, Fox JW, Aitken A, Pungercar J, Krizaj I (2003) The neurotoxic phospholipase A2 associates, through a non-phosphorylated binding motif, with 14-3-3 protein γ and ε isoforms. *Biochem Biophys Res Commun* **302:** 691–696

Tabrizi SJ, Orth M, Wilkinson JM, Taanman JW, Warner TT, Cooper JM, Schapira AH (2000) Expression of mutant α-synuclein causes increased susceptibility to dopamine toxicity. *Hum Mol Genet* **9:** 2683–2689

Ubl A, Berg D, Holzmann C, Kruger R, Berger K, Arzberger T, Bornemann A, Riess O (2002) 14-3-3 protein is a component of Lewy bodies in Parkinson's disease-mutation analysis and association studies of 14-3-3η. *Brain Res Mol Brain Res* **108:** 33–39

Vila M, Przedborski S (2004) Genetic clues to the pathogenesis of Parkinson's disease. *Nat Med* **10** (Suppl): S58–S62

Xu J, Kao SY, Lee FJ, Song W, Jin LW, Yankner BA (2002) Dopamine-dependent neurotoxicity of α-synuclein: a mechanism for selective neurodegeneration in Parkinson disease. *Nat Med* **8:** 600–606

Yaffe MB, Rittinger K, Volinia S, Caron PR, Aitken A, Leffers H, Gamblin SJ, Smerdon SJ, Cantley LC (1997) The structural basis for 14-3-3:phosphopeptide binding specificity. *Cell* **91:** 961–971

Yamamoto A, Friedlein A, Imai Y, Takahashi R, Kahle PJ, Haass C (2004) Parkin phosphorylation and modulation of its E3 ubiquitin ligase activity. *J Biol Chem* **280:** 3390–3399

Yao D, Gu Z, Nakamura T, Shi ZQ, Ma Y, Gaston B, Palmer LA, Rockenstein EM, Zhang Z, Masliah E, Uehara T, Lipton SA (2004) Nitrosative stress linked to sporadic Parkinson's disease: S-nitrosylation of parkin regulates its E3 ubiquitin ligase activity. *Proc Natl Acad Sci USA* **101:** 10810–10814

Zhong L, Tan Y, Zhou A, Yu Q, Zhou J (2005) RING finger ubiquitin-protein isopeptide ligase Nrdp1/FLRF regulates parkin stability and activity. *J Biol Chem* **280:** 9425–9430

Zhou W, Hurlbert MS, Schaack J, Prasad KN, Freed CR (2000) Overexpression of human α-synuclein causes dopamine neuron death in rat primary culture and immortalized mesencephalon-derived cells. *Brain Res* **866:** 33–43

THE JOURNAL OF BIOLOGICAL CHEMISTRY VOL. 281, NO. 6, pp. 3204–3209, February 10, 2006

Diverse Effects of Pathogenic Mutations of Parkin That Catalyze Multiple Monoubiquitylation *in Vitro*[*][S]

Received for publication, September 21, 2005, and in revised form, November 29, 2005 Published, JBC Papers in Press, December 8, 2005, DOI 10.1074/jbc.M510393200

Noriyuki Matsuda[‡], Toshiaki Kitami[§], Toshiaki Suzuki[‡], Yoshikuni Mizuno[§], Nobutaka Hattori[§], and Keiji Tanaka[‡1]

From the [‡]Laboratory of Frontier Science, Tokyo Metropolitan Institute of Medical Science, Bunkyo-ku, Tokyo 113-8613 and the [§]Department of Neurology, Juntendo University School of Medicine, 2-1-1 Hongo, Bunkyo-ku, Tokyo 113-0033, Japan

Mutational dysfunction of *PARKIN* gene, which encodes a double RING finger protein and has ubiquitin ligase E3 activity, is the major cause of autosomal recessive juvenile Parkinsonism. Although many studies explored the functions of Parkin, its biochemical character is poorly understood. To address this issue, we established an E3 assay system using maltose-binding protein-fused Parkin purified from *Escherichia coli*. Using this recombinant Parkin, we found that not the front but the rear RING finger motif is responsible for the E3 activity of Parkin, and it catalyzes multiple monoubiquitylation. Intriguingly, for autosomal recessive juvenile Parkinsonism-causing mutations of Parkin, whereas there was loss of E3 activity in the rear RING domain, other pathogenic mutants still exhibited E3 activity equivalent to that of the wild-type Parkin. The evidence presented allows us to reconsider the function of Parkin-catalyzed ubiquitylation and to conclude that autosomal recessive juvenile Parkinsonism is not solely attributable to catalytic impairment of the E3 activity of Parkin.

Recessive mutations in the human *PARKIN* gene are the most frequent cause of autosomal recessive juvenile parkinsonism, the common form of familial Parkinson disease (PD).[2] It has been shown that almost 50% of patients with familial autosomal recessive juvenile parkinsonism carry a series of exon rearrangements or point mutations in *PARKIN*. Moreover, recent findings of the haploinsufficiency of *parkin* and *S*-nitrosylation also imply its association in sporadic PD (1). The causal gene *PARKIN* encodes a double RING finger protein with ubiquitin ligase (E3) activity (2–5) and interestingly, missense mutations in the double RING finger motif resulted in an earlier onset of the disease than mutations in other function-unknown regions (6). To date, numerous biochemical studies have been performed to understand how mutations in Parkin lead to its dysfunction and to pathogenic outcome. However, because the biochemical characterization of E3 activity of Parkin has been difficult, it is still controversial whether the disease-relevant Parkin mutants lose their E3 activity or not. For example, one group of investigators implied that Parkin harboring K161N mutation loses its E3 activity (7), whereas another group suggested the same mutation dose not impair E3 activity (8). In the case of other PD mutations, the situation is even more complex (see supplemental Table 1). Thus, the mode of Parkin-catalyzed ubiquitylation remains poorly understood to date.

Little is known about the reconstituted ubiquitylating experiment using recombinant Parkin. Almost all of the biochemical analyses reported so far have been performed using *in vitro* translated Parkin or immunoprecipitated Parkin. However, it is difficult to avoid trace contaminants of other proteins that could physically interact with Parkin. Indeed it has been reported that Parkin interacts with other E3s such as CHIP (9) and Nrdp1/FLRF (10), and thus the results of experiments using immunoprecipitated or *in vitro* translated Parkin require careful interpretation. To study the E3 activity of intrinsic Parkin, a biochemical approach using bacterially expressed recombinant Parkin that is free from other contaminating E3 enzyme(s) is obviously required. We thus attempted to reconstitute a sensitive E3 assay system using Parkin purified from *Escherichia coli*.

EXPERIMENTAL PROCEDURES

Purification of Recombinant Proteins—To express Parkin in *E. coli*, it was important to use a modified *E. coli* strain BL21(DE3) codon-plus (RIL) strain (Stratagene, La Jolla, CA), because Parkin possesses many rare codons for *E. coli* that might cause low expression and/or amino acid misincorporation. For example, Parkin contains eight AGA codons that lead to mistranslation of lysine for arginine in *E. coli* (11). pMAL-p2T, in which the thrombin recognition site was inserted into pMALp2 (New England BioLabs, Beverly, MA), was prepared to purify maltose-binding protein (MBP)-LVPRGS-Parkin. Parkin cDNAs of wild type and various mutants/deletions were subcloned into BamHI site of pMAL-p2 and pMAL-p2T. All mutants/deletions were generated by PCR-mediated site-directed mutagenesis (details of the plasmid construction processes can be provided upon request). All recombinant fusion proteins were purified from bacterial lysate applying the method advocated by the supplier (New England BioLabs) using a column buffer containing 20 mM Tris-HCl, pH 7.5, 200 mM NaCl, 1 mM dithiothreitol, and 100 μM $ZnSO_4$. The eluted fraction containing 10 mM maltose was not dialyzed because Parkin tends to lose its E3 activity during dialysis. Instead, it was subjected to the ubiquitylation assay directly. We attempted to purify sole IBR-RING2 region of Parkin also by splitting MBP-IBR-RING2 (see "Results"). Specifically, we added E2, various detergents and stabilizers during the cleavage process expecting that they solubilize and/or stabilize free IBR-RING2 in solution. Even in all the above experimental conditions, however, we could not obtain soluble-free IBR-RING2 (data not shown). Six histidine-tagged proteins such as Uev1/Ubc13 were purified by the conventional method and dialyzed by a buffer containing 20 mM Tris-HCl, pH 8.0, 200 mM NaCl and 1 mM dithiothreitol. Glycerol of 6% was added as a stabilizer for preservation of recombinant MBP-Parkin and E2 proteins at −80 °C.

In Vitro Ubiquitylation Assay—The *in vitro* ubiquitylation assay was performed as described previously (12–14). Briefly, the purified MBP-Parkin (20 μg of MBP-Parkin/ml) was incubated in a reaction buffer (50

* This work was supported by grants-in-aid from the Ministry of Education, Culture, Sports, Science and Technology of Japan (to K. T.). The costs of publication of this article were defrayed in part by the payment of page charges. This article must therefore be hereby marked "*advertisement*" in accordance with 18 U.S.C. Section 1734 solely to indicate this fact.

[S] The on-line version of this article (available at http://www.jbc.org) contains supplemental Table 1 and Fig. 1.

[1] To whom correspondence should be addressed. Tel. and Fax: +81-3-3823-2237; E-mail: tanakak@rinshoken.or.jp.

[2] The abbreviations used are: PD, Parkinson disease; E1, ubiquitin-activating enzyme; E2, ubiquitin-conjugating enzyme; E3, ubiquitin ligase; GST, glutathione *S*-transferase; MBP, maltose-binding protein.

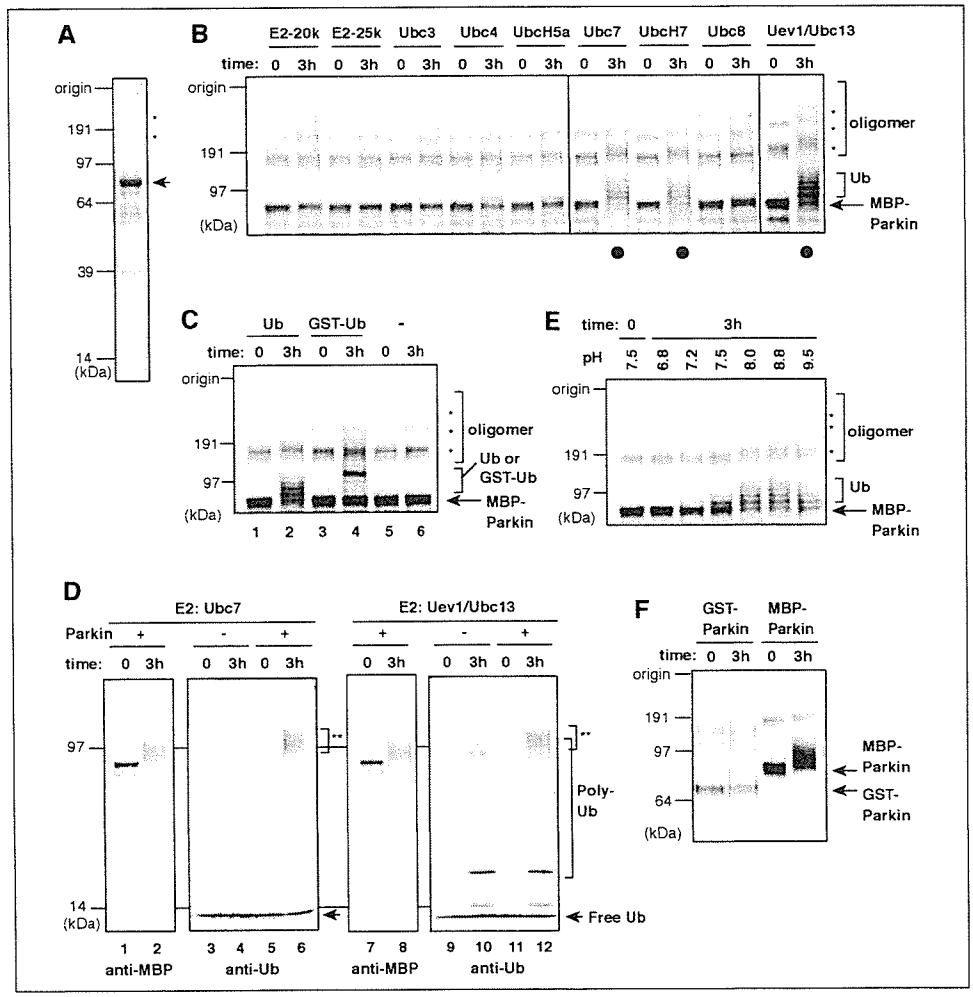

FIGURE 1. ***In vitro* ubiquitylation assay using Parkin derived from *E. coli*.** *A*, purified MBP-Parkin was visualized by CBB staining. The *arrow* indicates MBP-Parkin, and the *asterisks* indicate oligomerization bands. *B*, MBP-Parkin catalyzes autoubiquitylation in cooperation with Ubc7, UbcH7, and Uev1-Ubc13 (*solid circles*). MBP-Parkin was subjected to *in vitro* ubiquitylation assay and to immunoblotting with anti-MBP antibody. *Ub*, ladders derived from autoubiquitylation, *, oligomerization bands. *C*, confirmation of autoubiquitylation of MBP-Parkin. To demonstrate that the slower migrating ladders are because of autoubiquitylation, a reconstitution assay was repeated in the absence (−) or presence of ubiquitin (*Ub*) or GST-ubiquitin (*GST-Ub*). *D*, the high molecular weight forms of MBP-Parkin are recognized by anti-ubiquitin antibody. *Double asterisks* indicate the signal derived from MBP-Parkin autoubiquitylation. The *arrow* indicates free ubiquitin. *E*, Parkin prefers weak alkaline conditions to exert its E3 activity. *F*, GST-Parkin rarely exhibits E3 activity. Bacterial recombinant GST- and MBP-Parkin were concurrently subjected to ubiquitylation assay. Ubc7 was used as E2 in *C*, *E*, and *F*. Anti-MBP antibody was used in *B*, *C*, and *E*, and anti-Parkin antibody was used in *F*.

mM Tris-HCl, pH 8.8, 2 mM dithiothreitol, 5 mM $MgCl_2$, and 4 mM ATP) with 50 μg of ubiquitin/ml (Sigma), 1.6 μg of recombinant mouse E1/ml and 20 μg of purified E2 or 100 μg of various E2-expressing *E. coli* lysate/ml at 32 °C for 2 h and subjected to immunoblotting with anti-MBP antibody (New England BioLabs), anti-parkin (1A1) antibody (15), or anti-ubiquitin antibody (DakoCytomation, Carpinteria, CA). In some cases, GST-ubiquitin or methylated ubiquitin (BostonBiochem, Cambridge, MA) was used instead of native ubiquitin. The subsequent thrombin cleavage was performed by incubation on ice for 3 h in the presence of thrombin and 2 mM $CaCl_2$.

RESULTS

Autoubiquitylation by MBP-Parkin Fusion Protein—In 2001, Rankin *et al.* (16) reported that glutathione *S*-transferase (GST)-tagged Parkin purified from *E. coli* possesses E3 activity. However, we found that the E3 activity of this GST-Parkin is very weak (Fig. 1*F*), and thus there is a need for a more sensitive E3 assay system for bacterially expressed recombinant Parkin. During studies of other RING finger proteins, we recognized the superiority of the MBP-tag relative to GST-tag in purifying RING finger proteins that retain their E3 activities (12, 13, 17, 18) and hence decided to use MBP-Parkin. MBP-Parkin was purified using a modified *E. coli* strain BL21(DE3) codon-plus-RIL (Fig. 1*A*) and then incubated with ATP, ubiquitin, E1, and one of the E2 enzymes indicated in Fig. 1*B*, and we subjected it to immunoblotting with anti-MBP antibody. High molecular mass ladders derived from autoubiquitylation (see below) were observed when MBP-Parkin was incubated with Ubc7, UbcH7, and Uev1-Ubc13 (Fig. 1*B*, highlighted by the *solid circles*). Note that the slower migrating bands of more than 160 kDa observed even at reaction time zero (Fig. 1*B*, *asterisks*) or without ubiquitin (Fig. 1, *A* and *C*, *asterisks*) are derived from MBP-Parkin oligomerization. To test whether the modification acquired by MBP-Parkin is due to ubiquitylation, the same reaction products were subjected to immunoblotting with anti-ubiquitin antibody. When Ubc7 was used as E2 (Fig. 1*D*, *lanes 1–6*), only modified MBP-Parkin was detected by anti-ubiquitin antibody (*lane 6, double asterisks*), indicating that the modification acquired by MBP-Parkin was indeed autoubiquitylation. When Uev1-Ubc13 was used, a polyubiquitylation signal was observed even in the absence of MBP-Parkin (Fig. 1*D*, *lanes 9* and *10*), because Uev1-Ubc13 complex itself can catalyze polyubiquitin chain formation (19). Also in this case, modified MBP-Parkin reacted with anti-ubiquitin antibody, confirming the above conclusion (see Fig. 1*D*, *double asterisks* in *lane 12*; note that the difference between *lanes 10* and *12* corresponds to the autoubiquitylation signal of MBP-Parkin). Moreover, the replacement of ubiquitin with GST-ubiquitin retarded the mobility of these ladders (Fig. 1*C*, *lanes 3* and *4*), and the exclusion of ubiquitin completely quenched such ladders (Fig. 1*C*, *lanes 5* and *6*). Based on these results, we concluded that MBP-Parkin catalyzes autoubiquitylation in cooperation with Ubc7, UbcH7, and Uev1-Ubc13. Interestingly, autoubiquitylation became evident when the pH of the reaction buffer was increased to 8.0 and 8.8, indicating that Parkin prefers weak alkaline conditions to exhibit its E3 activity *in vitro* (Fig. 1*E*). Because MBP-Parkin possesses stronger E3